

INVESTIGATION OF THE ROLE OF NLRP13 IN CELL DEATH

by

Elif Öykü Çakır

B.S., Molecular Biology and Genetics, Middle East Technical University, 2019

Submitted to the Institute for Graduate Studies in
Science and Engineering in partial fulfillment of
the requirements for the degree of
Master of Science

Graduate Program in Molecular Biology and Genetics
Boğaziçi University

2022

ACKNOWLEDGEMENTS

Firstly, I would like to thank my supervisor Prof. Nesrin Özören for giving me the opportunity to work by admitting me to this lab. I am also grateful for her supervision and guidance during my master project for 2 years. I am thankful to my thesis committee members Assist. Prof. Necla Birgül İyison and Assoc. Prof. Ceren Çıracı for taking the time to evaluate my thesis.

I want to thank my very special labmates Ilke Süder, Hafize Ozen Kaya, Davod Khalafkhany, Efe Elbeyli, Sevgi Çıracı, Hilal Ok, Dilvin Berrak Güney and our intern İrem Ceren and hug them tightly. We were together with Sevgi and Hilal in whole this project. We went through the same paths together throughout the project, often falling into similar despair. I am grateful to both of them for making me feel that I am not alone in this way. I am thankful to İlke, Özen, Davod and Efe for being there whenever i need. I learned everything I know from them, moreover, I learned not only the techniques but also how to be a part of a lab. I want to thank the most kindred spirit and funniest intern İrem Ceren for our all laughter. The time I spent here was one of the best times of my life thanks to them. Thanks again to all of them for making even the hard days fun.

I want to thank specially Elif Çelik and Zeynep Ergün for helping me in flow cytometry and their eternal friendship and support. they never turned me down whenever I ask for a help and they were even more upset than me for every negative result. I am also thankful Ulduz Sophia Afshar for always helping me in many questions during this master project.

Additionally, I would like to thank Sütlü Lab, MTCRL (Yaman Lab), and Sumo Lab for providing the needed materials and equipment used in the experiments carried out for this thesis.

Special thanks to dear friends İrem Efe, İpek Öztürk, Begüm Savaş and Görkem Gence for all their supports during this adventure.

The one of the biggest thanks to my family Filiz Çakır, Gizem Altundağ, Sercan Kaya and especially my sister Naz İdil Çakır. I am grateful for being there whenever I fall, dealing with all my anxiety attacks, always understanding and not judging me. Another biggest thanks to myself for being such a super person.

ABSTRACT

INVESTIGATION OF THE ROLE OF NLRP13 IN CELL DEATH

NLRP13 is an intracellular protein that is included in the NOD-like receptor family. It contains the N-terminal pyrin domain, central NOD domain, and leucine-rich repeats, LRR at C terminus. Stably NLRP13 expressing THP-1 cells induced a higher pro-inflammatory response upon LPS/ATP treatment and *P. Aeruginosa* infection. Moreover, the activation of procaspase-8 is relatively increased in the stably NLRP13 expressing THP-1 cell. NLRP13 can interact with caspase-8 according to Co-IP results. Besides these, NLRP3 inflammasome components are significantly higher in the stably NLRP13 expressing THP-1 cells upon inflammasome activation. This thesis study aimed to investigate whether NLRP13 has a role in cell death via the caspase-8 activation complex after inflammasome activation. To elucidate this, Annexin V-PI staining and LDH release assay were performed after pyroptosis induction via inflammasome activation. No significant difference was observed between stably NLRP13 expressing THP-1 cells and control cells. Furthermore, Gasdermin D cleavage was shown to be similar for each group while PARP-1 cleavage in stably NLRP13 expressing THP-1 cells was slightly higher than control. The experiments were repeated after caspase-8 was inhibited. There was no significant difference in Annexin V-PI staining, LDH release assay, and gasdermin D cleavage. However, PARP-1 cleavage was slightly decreased in stably NLRP13 expressing THP-1 cells when caspase-8 was inhibited. It was shown that NLRP13 is not involved directly in pyroptosis via induction of the caspase-8 activation complex; however, it could be involved in the molecular switch mechanism between apoptosis and pyroptosis with the caspase-8 activation complex.

ÖZET

NLRP13'ün Hücre Ölümündeki Görevinin Araştırılması

NLRP13, NOD benzeri reseptör ailesine dahil olan hücre içi bir proteindir. N-terminal PYRIN bölgesi, NACHT bölgesi ve lösin bakımından zengin tekrarları, LRR'yi içerir. Stabil olarak NLRP13 eksprese eden THP1 hücrelerinde, LPS/ATP uygulaması ve *P. Aeruginosa* enfeksiyonu daha yüksek bir pro-inflamatuar yanıtı indükledi. Ayrıca, stabil NLRP13 eksprese eden THP-1 hücresinde procaspaz-8 aktivasyonunun nispeten arttığı ortaya çıktı. NLRP13, Co-IP sonuçlarına göre caspaz-8 ile etkileşime sahiptir. Bunların yanı sıra, NLRP3, caspaz-1 ve ASC gibi NLRP3 inflammatuar bileşenleri, inflammatuar aktivasyon üzerine stabil NLRP13 eksprese eden THP-1 hücreslerinde önemli ölçüde daha yüksektir. Bu tez çalışması, NLRP13'ün inflammatuar aktivasyon sonrası caspaz-8 aktivasyon kompleksi yoluyla hücre ölümünde rolü olup olmadığını araştırmayı amaçlamıştır. Bunu açıklamak için, THP-1 hücrelerinde inflammatuar aktivasyon yoluyla piroptoz indüksiyonundan sonra Annexin V-PI boyama ve LDH salınım deneyi yapıldı. Stabil olarak NLRP13 eksprese eden THP-1 hücreleri, yabancı tip hücreler ve kontrol hücreleri arasında önemli bir fark gözlenmedi. Ayrıca tüm gruplar için gasdermin D ve PARP-1 proteinlerinin kesilimi kontrol edildi. Gasdermin D kesilimi her grup için benzer olarak gösterilirken, stabil NLRP13 eksprese eden THP-1 hücrelerinde PARP-1 kesilimi kontrolden nispeten daha yüksekti. Her grupta caspaz-8 inhibe edildikten sonra deneyler tekrarlandı. Annexin V-PI boyamasında, LDH salınım tahlilinde ve gasdermin D bölünmesinde önemli bir fark yoktu. Bununla birlikte, caspaz-8 inhibe edildiğinde, stabil olarak NLRP13 eksprese eden THP-1 hücrelerinde PARP-1 bölünmesi biraz azaldı. NLRP13'ün caspaz-8 aktivasyon kompleksinin indüklenmesi yoluyla doğrudan piroptozda yer almadığı gösterilmiştir; ancak caspaz-8 aktivasyon kompleksi ile apoptoz ve piroptoz arasındaki moleküler geçiş mekanizmasında yer alabilir.

TABLE OF CONTENTS

ACKNOWLEDGEMENTS	iii
ABSTRACT	v
ÖZET	vi
LIST OF FIGURES	ix
LIST OF TABLES	xiii
LIST OF SYMBOLS	xiv
LIST OF ACRONYMS/ABBREVIATIONS	xv
1. INTRODUCTION	1
1.1. Cell Death	1
1.2. Apoptosis	1
1.3. Pyroptosis	3
1.4. Necrosis	4
1.5. Caspases	5
1.6. Caspase 8	5
1.7. Inflammasomes	6
1.8. NOD-Like Receptors	8
1.9. NLRP13	10
2. HYPOTHESIS AND PURPOSE	11
3. MATERIALS	12
3.1. Cell Lines	12
3.1.1. THP-1 Monocytic Cell Line	12
3.2. Chemicals and Plastics	12
3.3. Buffers and Solutions	13
3.3.1. Cell Culture	13
3.3.2. Western Blot	14
4. METHODS	21
4.1. Cell Culture	21
4.1.1. Maintenance of Cells	21
4.1.2. Treatments of PMA differentiated Macrophages	22

4.1.3.	Collection of Macrophages for Cell Viability Assays	22
4.2.	Western Blotting	23
4.3.	ELISA for IL1- β	24
4.3.1.	Preparation of Plates	24
4.3.2.	ELISA Assay Protocol	24
4.4.	LDH Release Assay	25
4.5.	Annexin V-PI Assay	25
4.6.	Statistical Analysis	26
5.	RESULTS	27
5.1.	The Effects of NLRP13 on Cell Death upon Inflammasome Activation .	27
5.1.1.	Induction of Pyroptosis via Inflammasome Activation	27
5.1.2.	Confirmation of Cell Viability	28
5.1.3.	Investigation of IL1- β Secretion upon Pyroptosis	33
5.1.4.	Investigation of Cell Death-Related Protein Levels upon Inflam- masome Activation	34
5.2.	The Effects of NLRP13 on Cell Death When Caspase 8 is Inhibited . .	37
5.2.1.	Investigation of Cell Viability When Caspase 8 is Inhibited . . .	37
5.2.2.	IL1- β Levels upon Pyroptosis in The Absence of Caspase 8 . . .	39
5.2.3.	Investigation of Cell Death-Related Proteins in Absence of Cas- pase8	40
6.	DISCUSSION	44
7.	References	49

LIST OF FIGURES

Figure 1.1.	Pyroptosis Mechanism	3
Figure 1.2.	Classification of the NLR gene family (Adapted from Zhong et al., 2013).	9
Figure 5.1.	Induction of Pyroptosis via LPS/Nigericin Treatment and Cell Viability. (a) Confirmation of NLRP13 expression in NLRP13 stable THP-1 cell by western blotting. (b) Treatment protocol to induce pyroptosis.(c) Cell viability of NLRP13 stable cells are significantly lower according to trypan blue staining. ****p<0.0001; mean \pm SD	28
Figure 5.2.	Stable NLRP13 expression does not have an effect on the cell death levels after inflammasome activation	29
Figure 5.3.	Cell Populations and Cell Death Percentage of NLRP13. (a) Q5 for PI staining shows the necrotic cell death, Q6 for double staining with PI and annexin V shows late-apoptotic and pyroptotic cell death, Q7 for annexin V staining shows early-apoptotic cell death, Q8 for double negative shows the viable cells. (b) Percentages of treated and untreated cells is calculated as total number of Q5, Q6 and Q7)	30
Figure 5.4.	Cell Populations and Cell Death Percentage of mCherry. (a) Q5 for PI staining shows the necrotic cell death, Q6 for double staining with PI and annexin V shows late-apoptotic and pyroptotic cell death, Q7 for annexin V staining shows early-apoptotic cell death, Q8 for double negative shows the viable cells. (b) Percentages of treated and untreated cells is calculated as total number of Q5, Q6 and Q7	31

Figure 5.5.	Cell Populations and Cell Death Percentage of wild-type. (a) Q5 for PI staining shows the necrotic cell death, Q6 for double staining with PI and annexin V shows late-apoptotic and pyroptotic cell death, Q7 for annexin V staining shows early-apoptotic cell death, Q8 for double negative shows the viable cells. (b) Percentages of treated and untreated cells is calculated as total number of Q5, Q6 and Q7	32
Figure 5.6.	Stable NLRP13 expression does not have an effect on the cell death levels after inflammasome activation	33
Figure 5.7.	Stable NLRP13 expression is significantly increased IL1- β Secretion after pyroptosis induction via inflammasome activation. **p < 0.01, ***p < 0.001 mean \pm SD	34
Figure 5.8.	GasderminD is cleaved after pyroptosis induction via inflammasome activation. (a) Protein levels of cleaved gasderminD and full length in treated N13, mCherry and WT. (b) Protein levels of cleaved gasderminD and full length in untreated N13, mCherry and WT. NT: Nontreated, N13: Stably NLRP13 expressing THP-1 cells, mCherry: Stably mCherry expressing THP-1 cells, WT: Wild-Type THP-1 cells.	35
Figure 5.9.	Stable NLRP13 expression does not affect cleaved gasderminD protein level.	35

- Figure 5.10. PARP-1 is cleaved after pyroptosis induction via inflammasome activation. (a) Protein levels of cleaved gasderminD and full length in treated N13, mCherry and WT. (b) Cleavage of PARP-1 in NLRP13 overexpressing cells is slightly higher than control group. NT: Nontreated, N13: Stably NLRP13 expressing THP-1 cells, mCherry: Stably mCherry expressing THP-1 cells, WT: Wild-Type THP-1 cells. * $p \leq 0.05$ mean \pm SD 36
- Figure 5.11. Caspase-8 inhibition is confirmed by Western Blotting. 37
- Figure 5.12. Cell Populations and Cell Death Percentages of N13, mCherry and WT. (a) Q5 for PI staining shows the necrotic cell death, Q6 for double staining with PI and annexin V shows late-apoptotic and pyroptotic cell death, Q7 for annexin V staining shows early-apoptotic cell death, Q8 for double negative shows the viable cells. (b) Percentages of treated and untreated cells is calculated as total number of Q5, Q6 and Q7 and Stable NLRP13 expression does not have an effect on cell death when caspase-8 is inhibited. N13: Stably NLRP13 expressing THP-1 cells, mCherry: Stably mCherry expressing THP-1 cells, WT: Wild-Type THP-1 cells. 38
- Figure 5.13. Stable NLRP13 expression does not have an effect on the cell death levels when caspase-8 is inhibited 39
- Figure 5.14. IL1- β secretion of NLRP13 overexpressing cells is higher than wild-type cells but not the control cells. N13: Stably NLRP13 expressing THP-1 cells, mCherry: Stably mCherry expressing THP-1 cells, WT: Wild-Type THP-1 cells. ** $p < 0.01$ mean \pm SD 40

Figure 5.15. Cleavage of gasderminD when caspase-8 is inhibited (a) Protein levels of cleaved gasderminD and full length without caspase-8 inhibition (b) Protein levels of cleaved gasderminD and full length when caspase-8 is inhibited WT. N13: Stably NLRP13 expressing THP-1 cells, mCherry: Stably mCherry expressing THP-1 cells, WT: Wild-Type THP-1 cells.	41
Figure 5.16. Stable NLRP13 expression does not affect the GasderminD protein level when caspase-8 is inhibited.	41
Figure 5.17. PARP-1 cleavage in caspase-8 inhibited cells and noninhibited cells. (a) Protein levels of cleaved PARP-1 and full length in inhibited N13, mCherry and WT. (b) Protein levels of cleaved PARP-1 and full length in noninhibited N13, mCherry and WT. N13: Stably NLRP13 expressing THP-1 cells, mCherry: Stably mCherry expressing THP-1 cells, WT: Wild-Type THP-1 cells.	42
Figure 5.18. Cleavage of PARP-1 in NLRP13 overexpressing cells is slightly lower than control group and significantly lower than WT when caspase-8 is inhibited. N13: Stably NLRP13 expressing THP-1 cells, mCherry: Stably mCherry expressing THP-1 cells, WT: Wild-Type THP-1 cells. * $p \leq 0.05$ **** $p_i 0.0001$; mean \pm SD . . .	43
Figure 6.1. Possible Roles of NLRP13 in Cell Death	45

LIST OF TABLES

Table 3.1.	Cell culture chemicals.	13
Table 3.2.	Western Blot Chemicals	14
Table 3.3.	Equipments	17
Table 3.4.	Antibodies	20
Table 3.5.	KITS	20
Table 4.1.	Chemicals for Treatments	22

LIST OF SYMBOLS

g	Gram
g	Gravity
kDA	Kilodalton
L	Liter
M	Molar
mg	Miligram
mM	Milimolar
mm	Milimeter
ml	Mililiter
min	Minute
ng	Nanogram
rpm	Revolutions per Minute
V	Volt
α	Alpha
β	Beta
γ	Gamma
δ	Delta
κ	Kappa

LIST OF ACRONYMS/ABBREVIATIONS

Ab	Antibody
AD	Acidic Transactivation Domain
APS	Ammonium Persulfate
ASC	Apoptosis Associated Speck-Like Protein Containing CARD
ATP	Adenosine Triphosphate
BIR	Baculoviral Inhibitory Repeat-like Domain
BSA	Bovine Serum Albumin
CARD	Caspase Activation and Recruitment Domain
Caspase	Cysteine-Aspartic Protease
CLR	C-type Lectin Receptor
DAMP	Danger Associated Molecular Patterns
DC	Dendritic Cell
dH ₂ O	Distilled water
ddH ₂ O	Double Distilled water
DMSO	Dimethyl Sulfoxide
DNA	Deoxyribonucleic Acid
EDTA	Ethylenediaminetetraacetic Acid
FADD	Fas-associated Protein with Death Domain
FBS	Fetal Bovine Serum
FC	Flow Cytometry
HBS	Hepes Buffer Saline
IL	Interleukin
LRR	Leucin Reach Repeat
LPS	Lipopolysaccharide
MHC	Major Histocompatibility Complex
NACHT	Present in NAIP, CIITA, HET-E, and TP1
NaCl	Sodium Chloride
NEAA	Non-essential Amino Acid
NLR	NOD-Like Receptor

NOD	Nucleotide-binding Oligamerization Domain
PAMP	Pathogen Associated Molecular Pattern
PBS	Phosphate Buffer Saline
PBS-T	Phosphate Buffer Saline and Tween 20
PFA	Paraformaldehyde
PMA	Phorbol 12-Myristate 13-Acetate
PRR	Pattern Recognition Receptor
PVDF	Polyvinylidene fluoride
PYD	Pyrin Domain
RLR	RIG-I-like Receptor
RNA	Ribonucleic Acid
RT	Room Temperature
SDS	Sodium Dodecyl Sulfate
SDS-PAGE	SDS-Polyacrylamide Gel Electrophoresis
TBS	Tris Buffered Saline
TBS-T	Tris Buffered Saline and Tween 20
TEMED	N,N,N',N'-Tetramethyl ethylenediamine
TLR	Toll Like Receptor
Tween 20	Polysorbate
V	Volume
w	Weight
WB	Western Blot
WT	Wild Type

1. INTRODUCTION

1.1. Cell Death

Cell death is a crucial event in organisms in terms of the disposal of damaged or unwanted cells. Cell death can occur through many different pathways due to various stimuli; however, it could be considered as two main types: accidental cell death (ACD) and regulated cell death (RCD). Accidental cell death is an uncontrolled process of cell death. Accidental cell death could be triggered via unexpected stimuli overwhelming the control mechanisms, such as physical or mechanical damage. On the other hand, regulated cell death depends on a strict molecular control mechanism. It includes signaling cascades, effector molecules, and several regulators. Moreover, this tightly controlled process leads to particular functional, biochemical, and immunological consequences. (Galluzzi et al., 2018)

Regulated cell death can also be subdivided into two groups based on its molecular characteristic; apoptotic cell death and non-apoptotic cell death.

1.2. Apoptosis

Apoptosis can be defined as the cell suicide process providing homeostasis and eliminating unwanted cells. It is strictly regulated by several signaling pathways since the balance between cell proliferation and death is crucial for all organisms. It is characterized by cytoplasmic shrinkage, DNA fragmentation, and the formation of membrane-bound apoptotic bodies phagocytosed rapidly to minimize the inflammation in contrast to pyroptosis. Caspase activation also has an essential role in apoptosis, similar to pyroptosis. There are two pathways of apoptosis: The extrinsic pathway and the Intrinsic pathway. (Tang et al., 2019)

Intrinsic apoptosis can be initiated by intracellular stimuli, including endoplasmic reticulum stress, DNA damage, ROS overload etc. Mitochondrial outer membrane permeabilization (MOMP) is a crucial and irreversible step of intrinsic apoptosis. The apoptosis regulator protein family (Bcl2) is responsible for its regulation of it. Bcl-2-associated X (BAX) or Bcl-2 antagonist killer (BAK) can mediate the mitochondrial outer membrane permeabilization in response to stimuli. They are only two of the Bcl-2 protein family that can form pores across the outer membrane of mitochondria. A variety of apoptosis-inducing conditions, including UV, reactive oxygen species (ROS), nitric oxide (NO), glucocorticoids, staurosporine treatment, BAX overexpression, and oncogenic stimuli such as c-MYC overexpression are known to cause a significant release of Cyt-c from the intermembrane space of mitochondria to the cytoplasm. The release of Cyt-c induces apoptosis through its interaction with APAF-1. A signaling complex called apoptosome is formed in the presence of dATP, Cyt-c, APAF-1, and pro-caspase-9. Pro-caspase 9 is activated as a part of the apoptosome complex and can cleave downstream effector caspases 3, 6, and 7. In other words, caspase-9 catalyzes the activation of caspase-3 and caspase-7, which are responsible caspases for apoptosis. (Özören & El-Deiry, 2003)

Extrinsic apoptosis is triggered by extracellular signals delivered in the form of ligands binding to death receptors. Death receptors are members of the tumor necrosis factor (TNF) superfamily and include TNF receptor-1 (TNFR1), CD95 (also called Fas and APO-1), death receptor 3 (DR3), TNF-related apoptosis-inducing ligand receptor (TRAIL). The binding of a ligand to a death receptor causes the monomeric pro-caspase 8 protein to be recruited via its DED to the death-inducing signaling complex (DISC) formed at the cytoplasmic tail of the engaged death receptor that also includes the adapter protein FAS-associated death domain (FADD) or TNFR-associated death domain (TRADD). Recruitment of caspase-8 monomers results in dimerization and activation. (Galluzzi et al., 2018)

1.3. Pyroptosis

Pyroptosis is a type of regulated cell death which is triggered by inflammasome activation. In other words, it could be defined as a consequence of inflammation. Based on the initiating stimulus, pyroptosis includes the activation of caspase-1, caspase-5 and caspase-11. Inflammasome activation is one of the features which distinguish of apoptotic cell death. There are also specific morphological features that are distinct from apoptotic cell death. Cell swelling and plasma membrane pores by the gasdermin protein family are some key features of pyroptosis. Besides, It leads to the secretion of several cytokines such as IL1- β and IL-18. Pyroptosis can be induced via two pathways: The caspase-1 dependent pathway and the Caspase-1 independent pathway. (Tang et al., 2019)

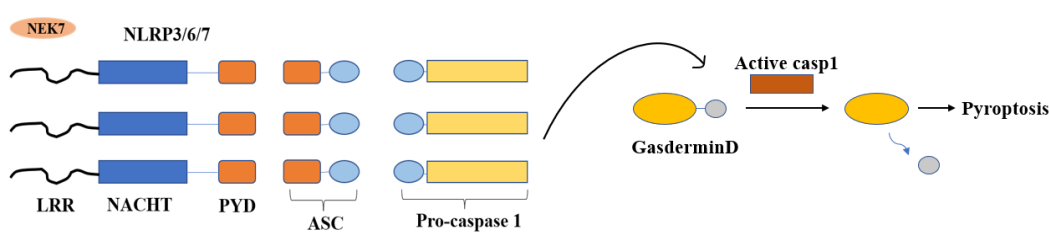


Figure 1.1. Pyroptosis Mechanism

Caspase-1 is required to cleavage gasdermin D protein in the caspase-1-dependent pathway. There are also two different pathways according to inflammasome, which are activated by different stimuli. When NLRP3 or AIM2 inflammasomes are activated by their stimuli, they recruit the ASC adaptor protein to interact with pro-caspase-1 and activate caspase-1. Then, caspase-1 causes the cleavage of gasdermin D resulting pyroptosis. Through this pathway, ASC adaptor protein is essential to induce pyroptosis; however, it is not required for the NLRC4 and NLRP1b inflammasomes. They can directly interact with pro-caspase-1 to form inflammasomes and activate caspase-1. Caspase-1 cleaves the gasdermin D protein resulting in pyroptosis. (Yu et al., 2021)

In the caspase-1 independent pathway, other caspases are required to cleavage gasdermin D instead of caspase-1, such as caspase-4/5/11. They can directly cleave the gasdermin D and induce pyroptosis. (Yu et al., 2021)

1.4. Necrosis

It is an uncontrolled cell death that results in swelling of the cell organelles, plasma membrane rupture and eventual lysis of the cell, and spillage of intracellular contents into the surrounding tissue leading to tissue damage. Unlike programmed cell death known as apoptosis which generates from intrinsic signals, necrosis occurs due to overwhelming noxious stimulus from outside the cell and is almost always associated with inflammatory responses due to the release of heat shock proteins, uric acid, ATP, DNA, and nuclear proteins, which cause inflammasome activation and secretion of pro-inflammatory cytokine interleukin-1 β (IL1- β). Typically, necrosis is not associated with caspase activation or normal development, but different types of regulated necrosis have been described, such as necroptosis. (Khalid & Azimpouran, 2022)

Necrotic cells release factors like high mobility group box 1 protein (HMGB1), and hepatoma-derived growth factor (HDGF). These factors are sensed by a nod-like receptor protein 3 (NLRP3), which is a core protein of the inflammasome. This results in inflammasome activation and causes the release of the pro-inflammatory cytokine IL1 β . is very common in vivo, mainly in diverse forms of neurodegeneration and death inflicted by ischemia or infection. Unlike unordered necrosis, necroptosis is a more physiological and programmed type of necroptotic death and shares several key processes with apoptosis. It occurs due to the activation of the kinase domain of the receptor-interacting protein 1 (RIP1) and the assembly of the RIP1/RIP3-containing signaling complex. It is triggered by tumor necrosis factor (TNF) family members, needs caspase 8 inhibition, and assembly of necrosome (RIPK1-RIPK3 complex IIb)

1.5. Caspases

Caspases are the family of cysteine-dependent proteases which have a critical role in regulating many types of cell death, including apoptosis and pyroptosis. They could be categorized into four groups; initiator caspases (Casp2, Casp8, Casp9, Casp10), effector caspases (Casp3, Casp6, Casp7), inflammatory caspases (Casp1, Casp4, Casp11, Casp12) and keratinization caspases (Casp14). (McIlwain et al., 2013)

In the cell, caspases are found in an inactive form, called procaspases, similar to many other proteases. Caspase 8 and caspase 10 contain four domains which are the small and large subunits, caspase activation and recruitment domain (CARD), death effector domain (DED) while casp1, casp2, casp4, casp5, casp9, and casp12 have only three domains except for death effector domain (DED). Effector caspases are cleaved into small and large subunits by other caspases to assemble into their active forms. (Li Yuan, 2008)

Inflammatory caspases involve in pyroptosis, whereas initiator and effector caspases have a role in the regulation of apoptosis. Caspase 3, caspase 6 and caspase 7 are required caspases for many types of apoptosis. Caspase 8 and caspase 9 are also required to activate them in extrinsic and intrinsic pathways. On the other hand, the cleavage of gasdermin family members by inflammatory caspases initiates the pore formation across the plasma membrane. (Zheng et al., 2020)

1.6. Caspase 8

Caspase-8 is a cysteine protease initiating the extrinsic apoptotic pathway in response to cell surface death receptor activation. Procaspase-8 is found in the cytosol within the cell as an inactive form, which is characterized by an N-terminal tandem death effector domains (DEDs) and a C-terminal catalytic protease domain. The activation of procaspase-8 is revealed to occur through an induced proximity mechanism. Upon interaction with the death ligand such as Fas Ligand, the clustering death receptor Fas recruits the adaptor protein Fas-associated death domain (FADD) to its

cytoplasmic tail.(Shen et al., 2018) The inactive pro-caspase-8 is recruited to FADD via homotypic interactions between the DEDs of procaspase-8 and the adaptor protein FADD, leading to the dimerization and activation of procaspase-8. The maturation of caspase-8 is derived by its auto-processing between p18 and p10 and subsequently between p18 and the pro-domain. The mature caspase-8 consists of two large subunits and two small subunits. (Ha et al., 2021)

Caspase-8 is involved in inflammation processes in a variety of ways: immune silent apoptosis induction through the cleavage of caspase-3 and bid; inflammation induction by processing IL-1 β and gasdermin D (GSDMD); inhibition of inflammatory cell death (necroptosis) by targeting Receptor-interacting protein kinase (RIPK)1, RIPK3 and cylindromatosis (CYLD). (Tummers Green, 2017)

Expression Caspase-8 seems to be downregulated in many cancer types such as breast cancer, colorectal cancer, hepatocellular carcinoma, prostate cancer, ovarian cancer, and neuroblastoma. (Tummers Green, 2017)

1.7. Inflammasomes

Inflammasomes are cytosolic multiprotein complexes involved in the innate immune response against pathogens. They can be activated via pathogen-associated molecular patterns (PAMPs) or danger-associated molecular patterns (DAMPs). Inflammasome formation contains a sensor protein, an inflammatory caspase, and an adaptor protein called apoptosis-associated speck-like protein containing CARD (ASC) in certain cases. Inflammasome activation is initiated by interaction between the sensor protein and its ligand. Different sensor proteins are known to form inflammasomes, such as NLRP3, NLRC4, NLRP7, NLRP12, AIM2 and PYRIN. (Latz et al., 2013)The formation of an inflammasome leads to cleavage of pro-caspase-1 into caspase-1, which is its active form. It converts the pro-IL-1 β and pro-IL-18 into IL-1 β and IL-18, their mature and active forms. Maturation of them is required for several immune reactions, such as the recruitment of innate immune cells to the infection site and interferon-gamma production. Moreover, activation of caspase-1 has a critical role in induc-

ing pyroptosis. Besides Casp-1, It was revealed that Casp-8, Casp-11, and receptor-interacting protein kinases have a role in contributing to the inflammasome function in some studies. In addition to the role of inflammasomes in defense mechanisms against pathogens, their formation can occur during physiological malfunctions. Thus, they could be involved in cancer development, metabolic, autoinflammatory, and neurodegenerative diseases. For example, mutations in the NLRP3 gene resulting in overactivation of the inflammasome formation were identified in patients with autoinflammatory diseases. Furthermore, many studies show that the NLRP3 inflammasome is activated in response to several neurological disorder-triggering molecules. While β -amyloid and α -synuclein, related to Alzheimer's and Parkinson's disorders, induce lysosomal rupture and Cathepsin B-dependent NLRP3 inflammasome activation; danger-associated molecular patterns during traumatic brain injury trigger ROS-dependent NLRP3 inflammasome activation. (Eren & Özören, n.d.) Inflammasome activation could occur via 2 different pathways; the canonical and non-canonical pathways. (Guo et al., 2015)

Canonical inflammasome activation requires NLRs, Caspase-1, and adaptor proteins ASC. NLRP1, NLRP3, NLRC4, and AIM-2 inflammasomes are known as well characterized. They can be sensed by different stimuli. For example, NLRP1 inflammasome is activated by lethal anthrax toxin from *Bacillus anthracis* while AIM2 is activated via DNA. (Zheng et al., 2020a) NLRP3 is the most studied inflammasome. It can sense various stimuli such as ATP, nigericin, and uric acid. The NLRP3 inflammasome needs two signals for activation. The first signal is a priming signal presented by stimulation of TLRs by LPS and induction of inflammasome components' gene expression through the NF κ B pathway. The second signal is an activatory signal that triggers the oligomerization of the complex NLRP3 with ASC and Caspase-1. It can be either ROS production by the mitochondria, potassium efflux resulting from ATP or Nigericin stimulation or lysosomal rupture triggered by phagocytosed crystals. (Eren & Ozoren et al., n.d.)

During the non-canonical inflammasome activation, human Casp-4,5 and mouse Casp-11 are found instead of caspase-1. A non-canonical NLRP3 inflammasome can be formed by Casp-11 against intracellular gram-negative bacteria. (Zheng et al., 2020a)

1.8. NOD-Like Receptors

Nucleotide-binding and oligomerization domain NOD-like receptors (NLRs) are cytosolic pattern recognition receptors of pattern-associated molecular patterns (PAMPs) and danger-associated molecular patterns (DAMPs). They have critical functions in examining the intracellular environment for the presence of infection and metabolic perturbations. In other words, they are required for the regulation of innate immunity. They can be found in macrophages, lymphocytes, dendritic cells, or non-immune cells, such as the epithelium. They are highly conserved. NLRs contain a central NACHT domain, a C-terminal leucine-rich repeat (LRR), and an N-terminal protein interaction domain. They are subdivided into four groups according to their effector domain; NLR-containing acidic transactivation domain (NLRA), NLR-containing baculoviral inhibitory like domain (NLRB), NLR-containing caspase recruitment domain (NLRC), and NLR-containing pyrin domain (NLRP). The NLRP subfamily contains 14 members, NLRP1-14. Six members in the NLC family contain CARD or CARD-related domains at the N-terminal, which are NLRC1, NLRC2, NLRC3, NLRC4, NLRC5, and NLRX1. NLRA and NLRB include only one member each. NLRA includes an AD domain and consists of a class II major histocompatibility complex transactivator. NLRB has a BIR domain; NLR family apoptosis inhibitory protein is its member. (Zhong et al., 2013)

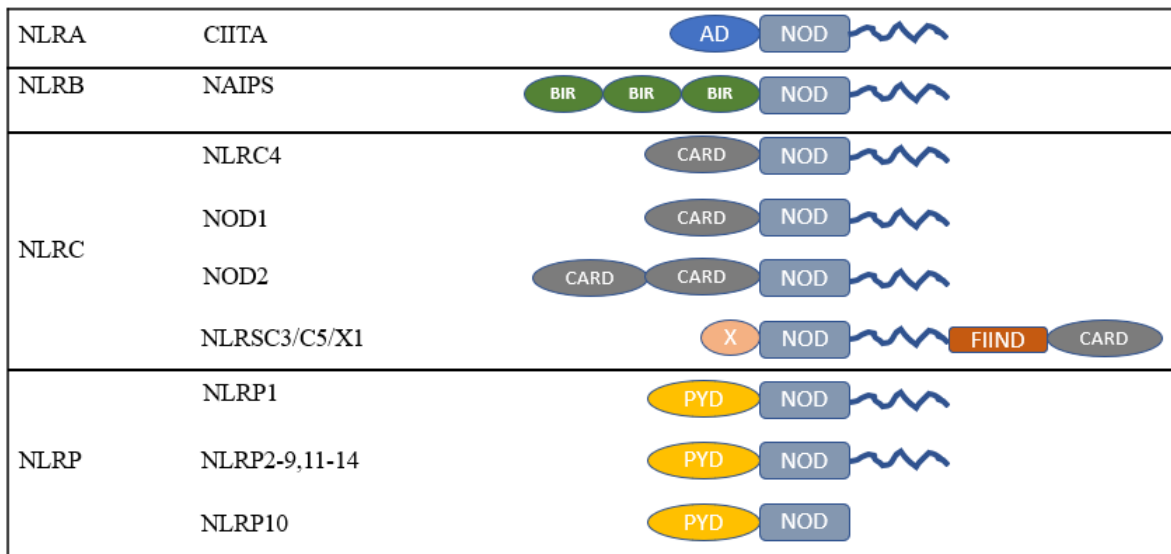


Figure 1.2. Classification of the NLR gene family (Adapted from Zhong et al., 2013).

NLRs mainly play a role in inflammasome assembly, signal transduction and cell death. They can induce inflammation and regulate pyroptosis by forming inflammasomes. They provide activation of the downstream pathways related to tumorigenesis, senescence, and immune responses in response to the received signal. (Zheng et al., 2020b) The NLRs recognize various ligands from microbial pathogens which are peptidoglycan, flagellin, viral RNA, fungal hyphae and host cells (ATPs, cholesterol crystals, uric acid) and environmental sources such as alum, asbestos, silica, alloy particles, UV radiation, skin irritants. When the eight NLRs (NLRP1, NLRP2, NLRP3, NLRP6, NLRP7, NLRP12, NLRC4, and NAIP) detect PAMPs and DAMPs, they recruit apoptosis-associated speck-like protein containing a CARD (ASC) via a pyrin-pyrin domain interaction. Subsequently, pro-caspase-1 binds to ASC through CARD-CARD domains, which completes the formation of an inflammasome. NOD1 and NOD2 activate the nuclear factor kappa B (NF- κ B) signaling pathway, which plays a significant role in regulating the host immune response. NOD1/NOD2 interact with a common downstream adaptor molecule called as receptor interacting protein 2 (RIP2), which is a serine/threonine kinase that can activate NF- κ B. Activated NF- κ B can move to the nucleus and enhance transcription of pro-inflammatory cytokines. On the other hand, NLRC3, and NLRP2/4 have a role as negative regulators of the NF- κ B pathway by modifying tumor necrosis factor (TNF) receptor-associated factor 6 (TRAF6).

Moreover, NLRA has a function in activation of MHC class II gene expression and NLRC5 plays a crucial role in the expression of the MHC class I gene. (Zhong et al., 2013)

1.9. NLRP13

NLR family pyrin containing 13, NLRP13, is an intracellular protein that is included in the NOD-like receptor family. Its molecular weight is 118 kD. It contains the N-terminal pyrin domain, NACHT domain, and leucine-rich repeats, LRR. It is known that it is only found in humans, dogs, bovines, and chimpanzees.

There are some mentions of it in the literature; however, there is no dedicated paper. These papers show the upregulation of the NLRP13 expression in THP-1 macrophages upon *Toxoplasma gondii* (Wang, 2016) and its survival in coinfection of HIV and tuberculosis. Another study shows that U87 glioblastoma cells that have resistance of doxorubicin in an invitro tumor microfluidic ecology, contain a missense mutation in NLRP13 gene(J. Han, 2016).

These findings were limited and insufficient to figure out the role of NLRP13 in inflammasome activation. Therefore, It was studied in our lab by former members. According to their studies, it was already known that NLRP13 is found in the cytosol and partly mitochondria, and it can weakly interact with inflammasome components; caspase-1 and ASC. (Gültekin, 2011) The increase in its expression upon LPS/ATP and *P. Aeruginosa* was also observed in the studies (Yalçinkaya, 2015; Yilmazer, 2018). Finally, it was indicated that NLRP13 shows a pro-inflammatory response upon LPS/ATP treatment and *P. Aeruginosa* infection. Moreover, it was revealed that cleaved subunits p43/p41 and p10 of caspase-8 are higher in the stably NLRP13 expressing THP-1 cells than control cells upon inflammasome activation. This means that activation of procaspase-8 is more increased in the stably NLRP13 expressing THP-1 cell. Furthermore, NLRP13 has an interaction with caspase-8 according to Co-IP results.

2. HYPOTHESIS AND PURPOSE

NLR family pyrin containing 13, NLRP13, is an intracellular protein that is included in the NOD-like receptor family. It contains the N-terminal pyrin domain, central NOD domain, and leucine-rich repeats, LRR at its C terminus. Formerly, The increase in its expression upon LPS/ATP treatment and *P. Aeruginosa* infection was also observed (Yalçinkaya, 2015; Yilmazer, 2018). NLRP13 shows a pro-inflammatory response upon LPS/ATP treatment and *P. Aeruginosa* infection as evident by higher levels of IL1- β , TNF- α have been detected in stably NLRP13 expressing human monocytic cell line THP-1. Moreover, it was revealed that activation of procaspase-8 is more increased in the stably NLRP13 expressing THP-1 cell. NLRP13 can interact with caspase-8 according to Co-IP results. Besides these, NLRP3 inflammasome components such as NLRP3, caspase-1, and ASC are significantly higher in the stably NLRP13 expressing THP-1 cells upon inflammasome activation (Yilmazer, 2018). Thus, it is possible that NLRP13 may activate caspase-1 and/or caspase-8.

The aim of this study is to investigate whether NLRP13 has a role in cell death by involving the caspase-8 activation complex after inflammasome activation. The stably NLRP13 expressing THP-1 cells and control cells were treated to induce the inflammasome to activate pyroptosis. Then, several cell death assays such as apoptosis, necrosis and pyroptosis and western blot were performed for this purpose.

Secondly, Caspase-8 inhibition were performed before the treatment. Then, cell death assays and Western blot were checked to understand whether NLRP13 has a role in cell death through the caspase-8 activation complex.

3. MATERIALS

3.1. Cell Lines

3.1.1. THP-1 Monocytic Cell Line

The THP-1 is a human monocytic cell line derived from acute leukemia. It was kindly provided by Prof Ahmet Gul of Istanbul University (Istanbul, Turkey) and grown in RPMI-1640 medium consists of 10% FBS, 100 U/ml penicilin, 100 $\mu\text{g}/\text{ml}$ streptomycin and 1X MEMNEA. Other cell culture chemicals are also listed in Table 3.1.

3.2. Chemicals and Plastics

Chemicals were purchased from Merck (Germany), Sigma (USA), or Applichem (Germany). Plastics were purchased from Axygen (USA), VWR (USA) or TPP (Switzerland). Before usage, the glassware, tubes and tips were autoclaved at 121°C for 20 minutes for sterilization. Other equipments are listed in Table 3.3.

3.3. Buffers and Solutions

3.3.1. Cell Culture

Table 3.1. Cell culture chemicals.

Chemicals	Supplier/Recipe
Dulbecco's Modified Eagled Medium	PAN Biotech, Germany
RPMI Media 1640	Gibco Invitrogen, USA
ATP	Sigma, USA
DMSO	Applichem, Germany
Puromycine	Sigma, USA
Fetal Bovine Serum	Gibco Invitrogen, USA
Penicilin/Streptomycin	Gibco Invitrogen, USA
PMA	Sigma, USA
LPS	Sigma, USA
MEM Non-essential amino acid 100X	Gibco Invitrogen, USA
PBS 10X	80 gr NaCl 2gr KCl 2.4 gr KH_2PO_4 14.4 gr Na_2HPO_4 Add ddH ₂ O up to 1 lt (pH:7.2)
PBS-EDTA	10 mM EDTA 1X PBS, pH: 8,0

3.3.2. Western Blot

Table 3.2 Western Blot Chemicals

Chemicals/Solutions	Supplier/Recipe
Acrylamide: Bisacrylamide	Applichem, Germany
Ammonium Persulfate	10% APS (w/v)
Blocking Solution	5% non-fat milk in TBS-T
Bovine Serum Albumin Fraction V	Roche, Germany
RIPA Buffer	25 mM Tris-HCl, pH:7,6 150 mM NaCl 1% NP-40 (w/v) 1% sodium deoxycholate (w/v) 0.1% SDS (w/v)
5X Laemmli Sample Buffer	1.25 M Tris-Hcl (pH:6,8) 5 mL 2-mercaptoethanol 5 mL 10% SDS 20 mL Glycerol 10 mL 0.5% bromophenol blue in ddH ₂ O 5 mL
2-Propanol	Merck, USA
Methanol	Merck, USA
SDS	Sigma-Aldrich, USA
TEMED	Merck, USA
4% Stacking Gel	3,3 mL Acrylamide Solution 6,3 mL 0,5 M Tris-HCl, pH:6,8 250 μ L 10% SDS (w/v) 15 mL ddH ₂ O
10% Stacking Gel	3,4 mL Acrylamide Solution 2,6 mL 2,6 M Tris-HCl, pH:8,8 100 μ L 10% SDS (w/v) 3,8 mL ddH ₂ O

Table 3.2 Western Blot Chemicals (Cont.).

15% Stacking Gel	5,0 mL Acrylamide Solution 6,3 mL 2,6 M Tris-HCl, pH:8,8 100 μ L 10% SDS (w/v) 2,2 mL ddH ₂ O
Pageruler Prestained Protein Ladder (26616)	Thermo Fisher Scientific, USA
PVDF Membrane	Merck, USA
10X TBS	24 g Tris-base 88 g NaCl up to 1 mL ddH ₂ O
1X TBS-T	1X TBS 1 L 1 mL Tween-20
10X Tris Glycine Buffer	30 g Tris-base 144 g Glycine up to 1 mL ddH ₂ O
1X Wet Transfer Buffer	100 mL 10X Tris Glycine Buffer 200 mL methanol up to 1 mL ddH ₂ O
Stripping Buffer (Mild)	7,5 g glycine 0,5 g SDS 20 mL Tween-20 up to 500 mL ddH ₂ O
WesternBright ECL HRP substrate	Advansta, USA
WesternBright Sirius HRP substrate	Advansta, USA
15% Stacking Gel	5,0 mL Acrylamide Solution 6,3 mL 2,6 M Tris-HCl, pH:8,8 100 μ L 10% SDS (w/v) 2,2 mL ddH ₂ O
Pageruler Prestained Protein Ladder (26616)	Thermo Fisher Scientific, USA
PVDF Membrane	Merck, USA

Table 3.2 Western Blot Chemicals (Cont.).

10X TBS	24 g Tris-base 88 g NaCl up to 1 mL ddH ₂ O
1X TBS-T	1X TBS 1 L 1 mL Tween-20
10X Tris Glycine Buffer	30 g Tris-base 144 g Glycine up to 1 mL ddH ₂ O
1X Wet Transfer Buffer	100 mL 10X Tris Glycine Buffer 200 mL methanol up to 1 mL ddH ₂ O
Stripping Buffer (Mild)	7,5 g glycine 0,5 g SDS 20 mL Tween-20 up to 500 mL ddH ₂ O

Table 3.3 Equipments

Autoclaves	MAC601, Eyela, Japan ASB260T, Astek, UK
Centrifuges	Allegra X22-R, Beckman, USA Himac CT4200C, Hitachi Koki, Japan J2-MC Centrifuge, Beckman, USA J2-21 Centrifuge, Beckman, USA
Freezers	2021D, Uğur, Turkey 4250T Uğur, Turkey
Flow Cytometer	BD Accuri C6, USA Sony Sh800 FACS Cell Sorter, Japan BD FACSymphony A5, USA
Incubator	PHC Europe B.V, The Netherlands
Heat Block	Thermal Shake lite, VWR, USA
Micropipettes	Rainin Mettler Toledo, USA Axygen, USA, Axypipettes, USA
Microscopes	Zeiss, Axio Observer, Germany Zeiss, Axio Observer Z1, Germany Nikon, Eclipse TS100, Netherlands
Microwave Oven	Arçelik, Turkey
Oven	Gallenkamp 300, UK
pH Meter	Hanna Instruments, USA
Pipettors	VWR, USA
Real-Time Quantitative PCR System	Longgene Q2000b, China
SDS-PAGE Electrophoresis System	Mini-Protean 4Cell BIO-RAD, USA
Power supply	Power Pac Universal, BIO-RAD, USA
SDS-PAGE Transfer Systems	Mini Trans-Blot Cell Trans-blot Semi-Dry BIO-RAD, USA

Table 3.3 Equipments (Cont.).

Shaker	Polymax USA Heildophl, Germany
Softwares	ImageJ, NIH, USA FlowJo, USA Syngene-Genetools, UK Leica LASX, USA
Spectrophotometer	Nanodrop ND-100 Thermo, USA
Tube Rotator	Globe Scientific, USA
Thermal Cyclers	BIO-RAD, USA
Vortex	GmcLab, Gilson, USA
Water Bath	GFL, Germany
Water filter	UTES, Turkey
Western Blot and Agarose Gel Visualization	Syngene GBOX, UK
Autoclaves	MAC601, Eyela, Japan ASB260T, Astekk, UK
Centrifuges	Allegra X22-R, Beckman, USA Himac CT4200C, Hitachi Koki, Japan J2-MC Centrifuge, Beckman, USA J2-21 Centrifuge, Beckman, USA
Freezers	2021D, Uğur, Turkey 4250T Uğur, Turkey
Flow Cytometer	BD Accuri C6, USA Sony Sh800 FACS Cell Sorter, Japan BD FACSymphony A5, USA
Incubator	PHC Europe B.V, The Netherlands
Heat Block	Thermal Shake lite, VWR, USA
Micropipettes	Rainin Mettler Toledo, USA Axygen Axygen, USA, Axypipettes, USA
Microscopes	Zeiss, Acio Observer, Germany

Table 3.3 Equipments (Cont.).

Microwave Oven	Arçelik, Turkey
Oven	Gallenkamp 300, UK
pH Meter	Hanna Instruments, USA
Pipettors	VWR, USA
Real-Time Quantitative PCR System	Longgene Q2000b, China
SDS-PAGE Electrophoresis System	Mini-Protean 4Cell BIO-RAD, USA
Power supply	Power Pac Universal, BIO-RAD, USA
SDS-PAGE Transfer Systems	Mini Trans-Blot Cell Trans-blot Semi-Dry BIO-RAD, USA

Table 3.4. Antibodies

Antibodies	Host	Supplier	Application
NLRP13 (ab105410)	Rabbit	Abcam, UK	WB
Caspase-8 (1C12)	Mouse	CST, USA	WB
GAPDH (14C10)	Rabbit	CST, USA	WB
Beta-Actin (13E5)	Rabbit	CST, USA	WB
Gasdermin D (E9S1X)	Rabbit	CST, USA	WB
PARP (46D11)	Rabbit	CST, USA	WB

Table 3.5. KITS

Chemicals	Supplier
LDH Release Assay	Roche, Switzerland
FITC Annexin V Apoptosis Detection Kit I (RUO)	BD, USA
IL1-B ELISA kit	BD USA

4. METHODS

4.1. Cell Culture

4.1.1. Maintenance of Cells

THP-1 cells were grown in an RPMI-1640 medium containing 10% FBS, 1% penicillin-streptomycin, and 1% MEMNEA. They were maintained in an incubator at 37°C with 5% CO₂.

The cells were taken at approximately 1/5 ratio and centrifuged at 1000 rpm for 5 min to subculture. Then, they were resuspended in the fresh medium. Or, 80% of the medium was removed directly from the flask, and fresh medium was added. The cells were subcultured every three days.

For freezing the cells, they were resuspended with 1 ml of 40% complete medium, 50% FBS, and 1% DMSO gently after centrifugation at 1000 rpm for 5 min. They were kept in cryotubes at -80°C or -150°C

For thawing the cells, cryotubes taken from -80 were incubated in the water bath for a short time. Then, the cell suspension was quickly diluted with 4 ml of complete medium. After centrifugation, the cells were resuspended in 20% FBS containing RPMI.

4.1.2. Treatments of PMA differentiated Macrophages

THP-1 cells were seeded to a 6-well plate as 1.5×10^6 cells per well. They were differentiated into m0 macrophages via 10 ng/ml PMA treatment for 24 hours. After 24h, the medium was changed, and the cells were left to allow differentiation for 24h. Then, they were treated with many different substances listed in Table 4.1 to induce pyroptosis and apoptosis.

Table 4.1. Chemicals for Treatments

Chemicals	Supplier/Recipe
PMA	10 ng
LPS	100 ng
Nigericin	10uM
Caspase-8 inhibitor Z-IETD-FMK	20uM

4.1.3. Collection of Macrophages for Cell Viability Assays

Medium of the treated cells was carefully collected into eppendorfs for cytokine detection and LDH release assay. The attached cells were incubated with cold 10mM EDTA in PBS on ice for 45 min. 45 min later, cells were detached by gentle pipetting and checked under a microscope to see whether they were detached or not. After they were removed into a falcon, plates were also washed with cold PBS twice to collect whole cells in the plates. Then, cells were centrifuged at 1000 rpm for 5 min. Supernatant was carefully removed and pellet was kept as sample. Some of them was used for flow cytometry or trypan blue staining and some of them was stored as lysate.

4.2. Western Blotting

RIPA solution was added to collected cells as 400ul per 1 million cells. Samples with RIPA were incubated at -20°C for an hour. Then, 5X laemli was added to samples with a final concentration of 1X. Proteins were denatured at 95C for 10 min. SDS gels consist of 10% 12% or 15% resolving and 4% stacking parts in 1.5mm glasses. Denatured samples were loaded into wells in the gel and run in the tank filled with 1X running buffer at 80V for a while; then, it increased to 120V. After running, the gel was transferred to the PVDF membrane by using the wet transfer method. The membrane was activated with methanol and washed with ddh₂o. Whatmann, sponges, and other materials required for the transfer were kept in the wet transfer buffer. For the transfer, sponge, whatmann, gel and membrane were placed as a sandwich, respectively. The sandwich was placed into the tank filled with 1X wet transfer buffer and transferred at 100V for 3 hours. After completing it, the membrane was blocked with 5% non-fat milk in TBS-T at room temperature for an hour. It was washed with TBS-T three times before incubation with a 1:1000 primary antibody (given in table 3.4), which is dissolved in 5% BSA in TBST. It was incubated in a 50ml falcon on the rotator overnight at 4°C degrees. The membrane was washed with TBT-T three times and placed into a 1:5000 HRP-linked secondary antibody (given in table 3.4) for incubation for an hour at room temperature. For the imaging, Syngene Genetools was used.

4.3. ELISA for IL1- β

4.3.1. Preparation of Plates

One day before, 96 well microplates were coated with capture antibody supplied from the kit given in Table 3.5 as 100 μ l per well in a working concentration overnight at room temperature. After overnight incubation, the capture antibody was removed and plates were washed with 300 μ l PBS-T per well three times. Plates were tapped into clean towels in every wash step to eradicate the buffer. The washed plates were blocked with 300 μ l reagent diluent containing 1% BSA in PBS-T for an hour at room temperature. Then, they were rewashed three times.

4.3.2. ELISA Assay Protocol

After blocking for 1h, the samples were diluted at 1:100 to keep the absorbance in the range of the standards. Dilutions of them and standards supplied from the kit were prepared and placed into wells. They were incubated for 2h at room temperature. The detection antibody was prepared at a working concentration when incubation was completed. The samples were removed from the plate. The plate was washed with 300 μ l PBS-T three times by tapping into clean towels to decrease the background. Then, it was incubated with a 100 μ l detection antibody supplied from the kit for 2h at room temperature. It was rewashed three times, and 100 μ l streptavidin-HRP was added to each well. It was covered to avoid light at this step for 20 min. After 20 min incubation, stop solution was added into wells immediately to avoid background signal. Then, plates were read by Plate Reader at A_{450} - A_{540} . Concentrations was calculated according to standard curve.

4.4. LDH Release Assay

The assay was performed according to instructions in the kit given in Table 3.5. Treatments were done in RPMI without FBS and phenol red because they create color change during assay protocol to lead background. Therefore, the medium collected from cells should not contain FBS or phenol red. 100 ul medium was loaded into a 96-well microplate. Untreated groups were used as low control groups. RPMI medium without FBS and phenol red was used as a blank. An equal number of cells were treated with 2% Triton-X as high control. Finally, catalyst and dye solution were mixed as working concentrations and 100 ul mixture solution was added to each well by avoiding light. It was incubated for up to 30 min. Plate was read in the plate reader at absorbance (490-600 nm). Percentages were calculated according to equation below.

$$\frac{(Sample - Blank) - (LowControl - Blank)}{(HighControl - Blank) - (LowControl - Blank)} \times 100$$

4.5. Annexin V-PI Assay

The cells were treated the completely same way. The cells were collected as 200.000 for each group and washed with 1X PBS twice. They were resuspended in 1X binding buffer by a vortex. They were incubated with 5 ul PI and 5 ul Annexin V for 15 min avoiding light according to kit given Table 3.5 instructions. Unstained THP-1 cells were used as a negative control. The cells were also stained with only PI and only annexin V separately as a single stain to take the gate properly for each. Samples were read by Calibur flow cytometry. Gates were taken according to population for each group. Then, analysis performed in FlowJo.

4.6. Statistical Analysis

The statistical analyses were performed with GraphPad Prism 8 (San Diego, USA). At graphs, the data were demonstrated as mean \pm standard deviation. For analysis multiple compared was applied following 2way ANOVA. Significance was presented as * $p \leq 0.05$, ** $p < 0.01$, *** $p < 0.001$, **** $p < 0.0001$.

5. RESULTS

5.1. The Effects of NLRP13 on Cell Death upon Inflammasome Activation

5.1.1. Induction of Pyroptosis via Inflammasome Activation

To investigate the effects of NLRP13 on cell death, stably NLRP13 expressing THP-1 cells were thawed from -80°C . Their lysates were collected and western blotting was performed to check whether their NLRP13 expression is still consistent or not. Wild type THP-1 monocytic cells were used as a negative control in the western blot analysis. The thick band in the figure 5.1a confirms that NLRP13 expression in the stably NLRP13 expressing THP-1 cells was still consistent (Figure 5.1a). After that, three experimental groups, wild type, NLRP13, and mCherry as a control group, were used. 1.5×10^6 THP-1 cells were seeded on a 6-well plate for each group and their untreated control groups. To induce pyroptosis via inflammasome activation, the treatment protocol shown in the figure 5.1b was performed for each group except for the untreated control group. Firstly, PMA was given to them for 24h. After 24h PMA treatment, their medium was changed and left to rest for 24h. The cells were primed with LPS for 4h and then nigericin was added to each well for 2h. Samples were collected with PBS containing EDTA buffer without using any scraper to prevent cells die. The collected samples were stained with trypan blue and counted by a cell counter to observe the cell viability. The cell viability of untreated cells was measured quite similar for all groups and it was around 95% as shown in the figure 5.1c. However, the cell viability of treated stably NLRP13 expressing THP-1 cells was almost less than half compared with our control group, mCherry (Figure 5.1c) It was shown that stably NLRP13 expressing cells died more than the control group after the LPS/nigericin treatment. (Figure 5.1c)

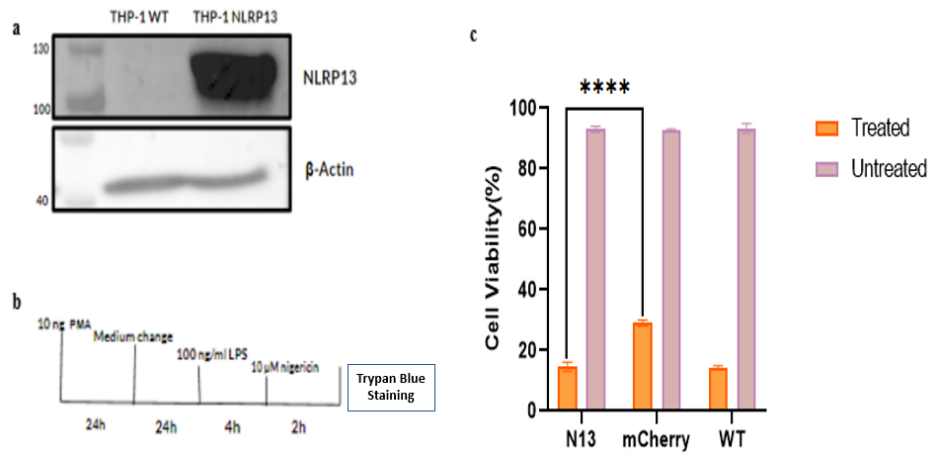


Figure 5.1. Induction of Pyroptosis via LPS/Nigericin Treatment and Cell Viability.

(a) Confirmation of NLRP13 expression in NLRP13 stable THP-1 cell by western blotting. (b) Treatment protocol to induce pyroptosis. (c) Cell viability of NLRP13 stable cells are significantly lower according to trypan blue staining. **** $p < 0.0001$; mean \pm SD

5.1.2. Confirmation of Cell Viability

To check cell death levels, we decided to evaluate cell viability using lactate dehydrogenase levels. After treatment as given in figure 5.1b, the medium of the cells was collected, and all cells were removed by centrifugation to obtain a cell-free medium. A high control, low controls and treated groups were placed into a 96-well microplate in triplicates. LDH release assay was performed according to the instructions of the kit and plates were read by Plate Reader. The LDH release percentage was calculated for each group and the results are shown as similar for stably NLRP13 expressing cells, mCherry expressing control cells and wild type cells. (Figure 5.2)

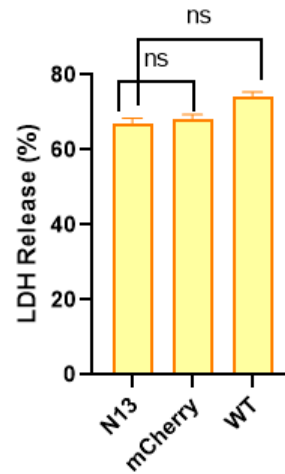


Figure 5.2. Stable NLRP13 expression does not have an effect on the cell death levels after inflammasome activation

To investigate apoptosis induction after inflammasome activation, Annexin V-PI staining was also performed for both treated and untreated groups to investigate different cell death types after pyroptosis induction. The cells were treated the completely same way as given in figure 5.1b. The cells were collected as 200.000 for each group and washed with 1X PBS twice. They were resuspended in 1X binding buffer. They were incubated with PI and Annexin V for 15 min avoiding light. Unstained THP-1 cells were used as a negative control. The cells were also stained with only PI and only annexin V separately as a single stain to take the gate properly for each. Samples were read by Calibur flow cytometry. Gates were taken according to population for each NLRP13 expressing THP-1 cells, mCherry expressing THP-1 cells and wild type THP-1 cells shown in the figure 5.3a, 5.4a and 5.5a respectively. X-axis shows the annexin V which is found in FL1 channel while Y-axis shows PI which is found in the FL2 channel. Only PI positive cells, shown in quadrant 5 (Q5), indicate the necrotic cells while only annexin V positive cells, shown in quadrant 7 (Q7), indicate the early-apoptotic cells. Double positive cells in quadrant 6 (Q6) are shows late-apoptotic and pyroptotic cells. Finally, cells in the quadrant 8 (Q8) are double negative cells and this indicates the viable cells. Cell death was calculated as total percentage of Q5, Q6 and Q7 for each NLRP13 THP-1 cells, mCherry THP-1 cells and wild type THP-1 cells as given in figure 5.3b, 5.4b and 5.5b. When the percentage of cell death of NLRP13

expressing cells compared with our control group mCherry and wild types THP-1 cells, no significant difference was not detected (Figure 5.6).

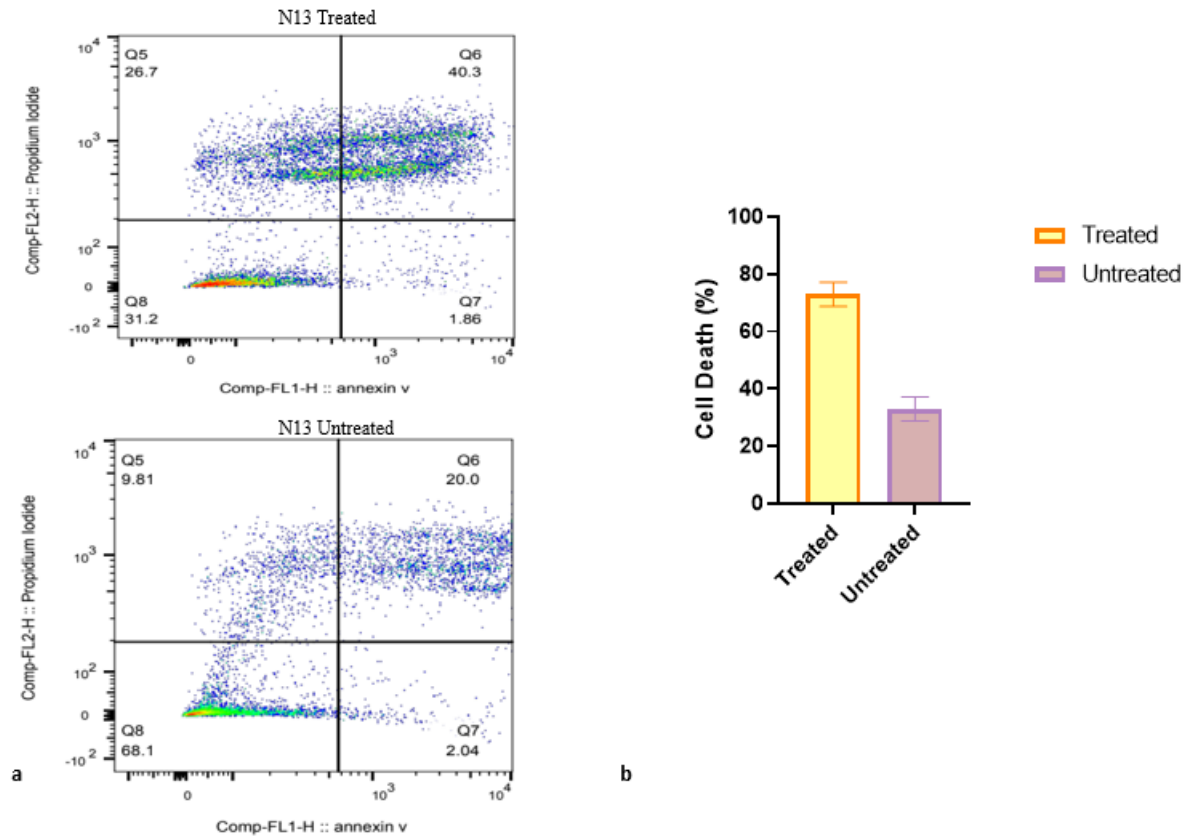


Figure 5.3. Cell Populations and Cell Death Percentage of NLRP13. (a) Q5 for PI staining shows the necrotic cell death, Q6 for double staining with PI and annexin V shows late-apoptotic and pyroptotic cell death, Q7 for annexin V staining shows early-apoptotic cell death, Q8 for double negative shows the viable cells. (b) Percentages of treated and untreated cells is calculated as total number of Q5, Q6 and Q7)

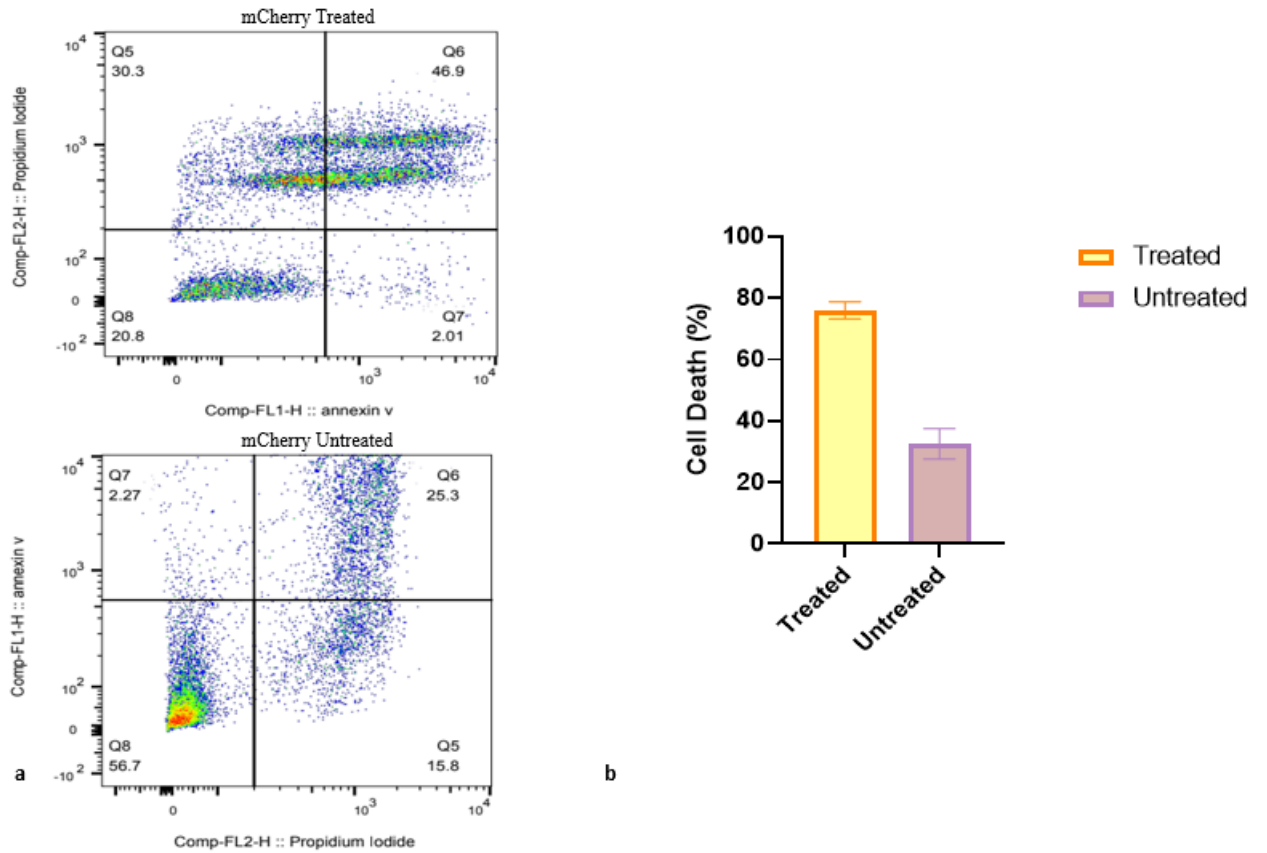


Figure 5.4. Cell Populations and Cell Death Percentage of mCherry. (a) Q5 for PI staining shows the necrotic cell death, Q6 for double staining with PI and annexin V shows late-apoptotic and pyroptotic cell death, Q7 for annexin V staining shows early-apoptotic cell death, Q8 for double negative shows the viable cells. (b) Percentages of treated and untreated cells is calculated as total number of Q5, Q6 and Q7

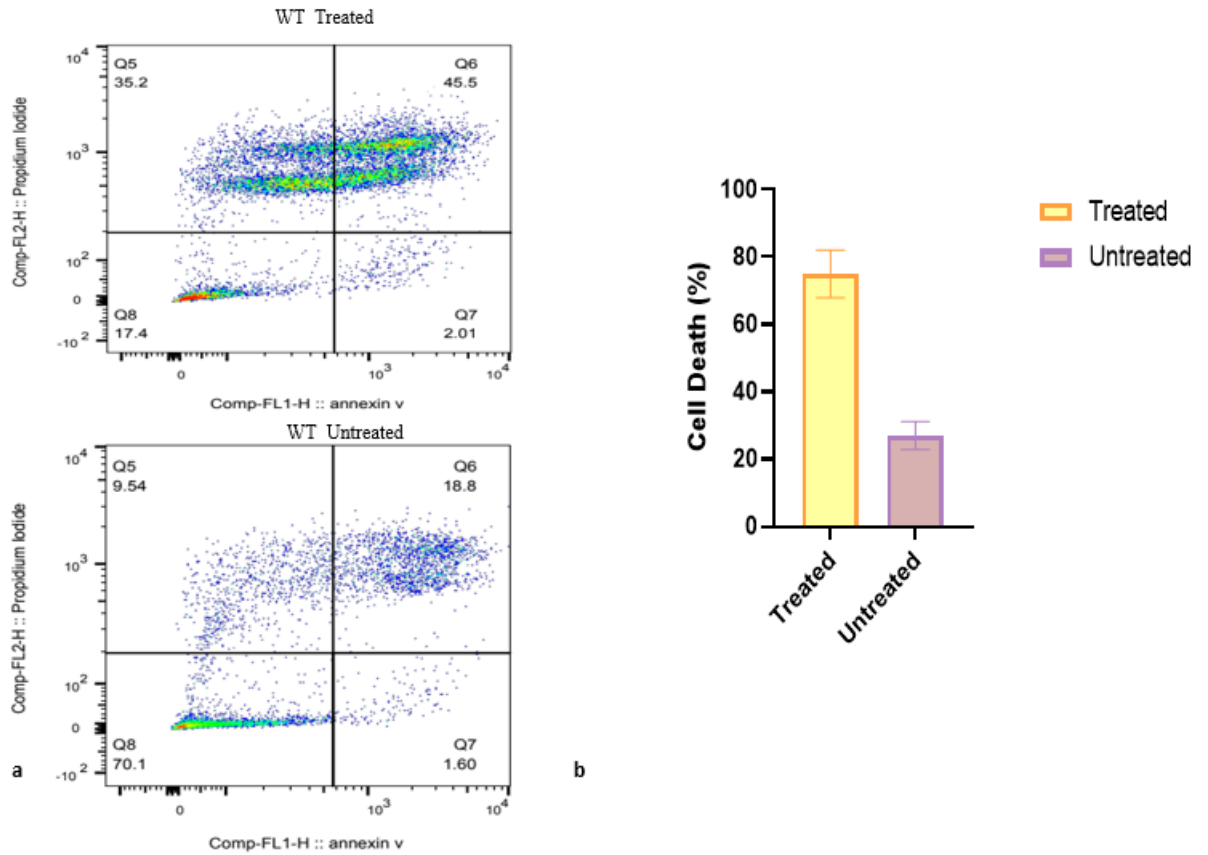


Figure 5.5. Cell Populations and Cell Death Percentage of wild-type. (a) Q5 for PI staining shows the necrotic cell death, Q6 for double staining with PI and annexin V shows late-apoptotic and pyroptotic cell death, Q7 for annexin V staining shows early-apoptotic cell death, Q8 for double negative shows the viable cells. (b) Percentages of treated and untreated cells is calculated as total number of Q5, Q6 and Q7

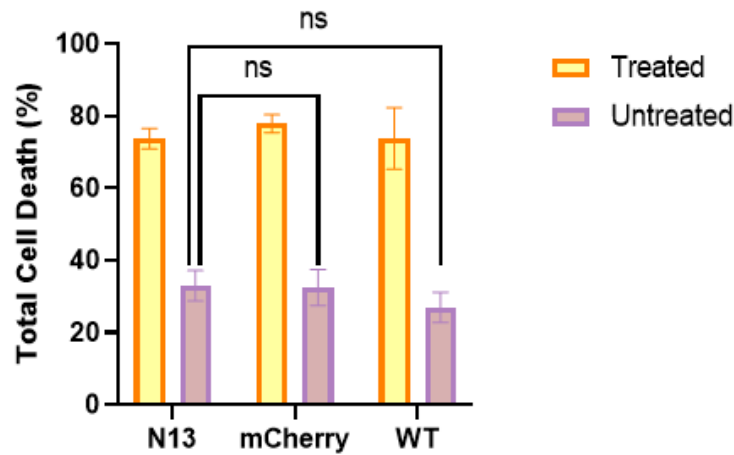


Figure 5.6. Stable NLRP13 expression does not have an effect on the cell death levels after inflammasome activation

5.1.3. Investigation of IL1- β Secretion upon Pyroptosis

IL1- β secretion is one of the critical indicators of inflammasome activation and pyroptosis. Therefore, the change of the IL1- β levels after pyroptosis induction was checked by ELISA. The medium of all groups was collected for ELISA analysis. The medium of treated groups was diluted as 1:100 to keep the absorbance between the range of standard solutions. They were put into a 96-well microplate, and the standard solution was also placed and diluted as serial dilution for incubation for 2h. Then, the detection antibody was prepared at a working concentration. The samples were removed from the plate. Streptavidin-HRP was added to each well. It was covered to avoid light at this step. After the assay was completed, the plate was read by a plate reader at A_{450} - A_{540} . Then, concentration of β was calculated according to standards. The highest concentration belonged to NLRP13 stable THP-1 cells. The IL1- β concentration of stably NLRP13 expressing THP-1 cells was observed as significantly higher than both mCherry and wild-type groups. (Figure 5.7)

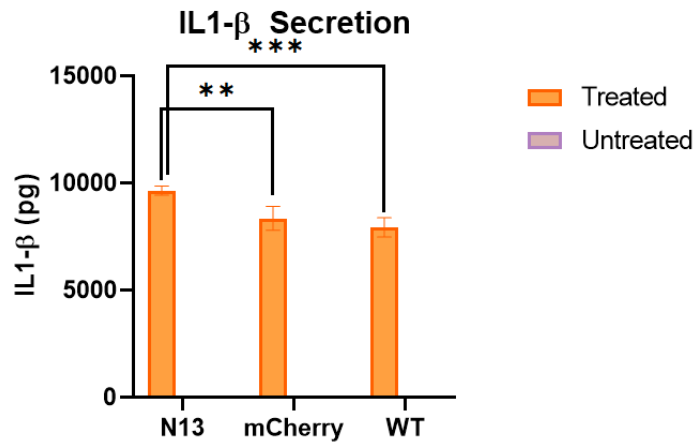


Figure 5.7. Stable NLRP13 expression is significantly increased IL1- β Secretion after pyroptosis induction via inflammasome activation. ** $p < 0.01$, *** $p < 0.001$ mean \pm SD

5.1.4. Investigation of Cell Death-Related Protein Levels upon Inflammasome Activation

Another critical indicator of pyroptosis is GasderminD cleavage since it is a downstream target of caspase-1 and caspase-8 in some cases. It should be cleaved by caspases to induce pyroptosis. Therefore, gasderminD full length and its cleaved form were checked via western blot analysis. All samples were loaded into the gel with an equal volume. Cleavage of gasderminD seemed to occur in all treatment groups successfully, while there was no cleavage in the untreated groups as expected (Figure 5.8). When western blot results were quantified by ImageJ, there was no significant difference in cleavage according to 2way ANOVA test. (Figure 5.9)

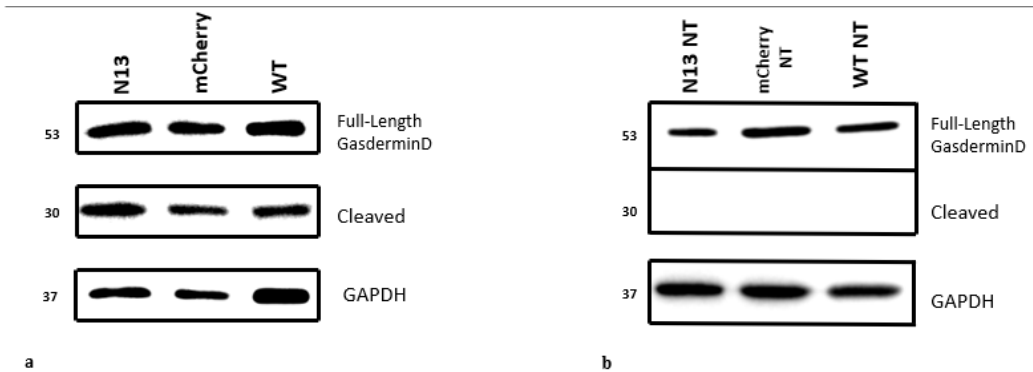


Figure 5.8. GasderminD is cleaved after pyroptosis induction via inflammasome activation. (a) Protein levels of cleaved gasderminD and full length in treated N13, mCherry and WT. (b) Protein levels of cleaved gasderminD and full length in untreated N13, mCherry and WT. NT: Nontreated, N13: Stably NLRP13 expressing THP-1 cells, mCherry: Stably mCherry expressing THP-1 cells, WT: Wild-Type THP-1 cells.

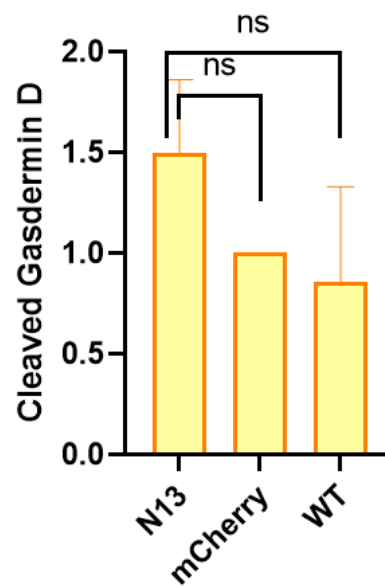


Figure 5.9. Stable NLRP13 expression does not affect cleaved gasderminD protein level.

There are several apoptosis-related proteins, and one of them is PARP-1. PARP-1 cleavage is an essential indicator of apoptosis. To check whether there is a difference in the PARP-1 cleavage levels between groups, western blot analysis was performed for all groups and quantified by ImageJ. Its cleavage was observed in all treated cells. (Figure 5.10a) Cleavage of PARP-1 is slightly higher in stably NLRP13 expressing THP-1 cells than the control group mCherry according 2way ANOVA test (Figure 10b).

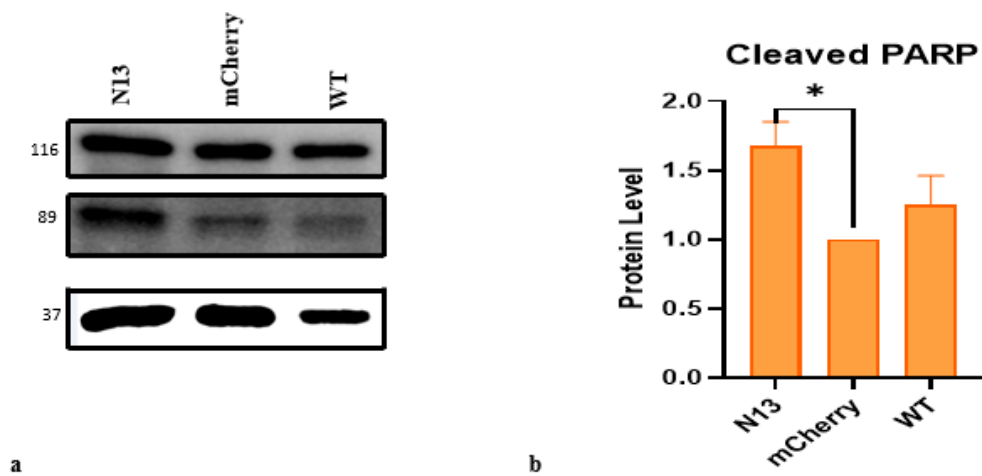


Figure 5.10. PARP-1 is cleaved after pyroptosis induction via inflammasome activation. (a) Protein levels of cleaved gasderminD and full length in treated N13, mCherry and WT. (b) Cleavage of PARP-1 in NLRP13 overexpressing cells is slightly higher than control group. NT: Nontreated, N13: Stably NLRP13 expressing THP-1 cells, mCherry: Stably mCherry expressing THP-1 cells, WT: Wild-Type THP-1 cells. * $p \leq 0.05$ mean \pm SD

5.2. The Effects of NLRP13 on Cell Death When Caspase 8 is Inhibited

5.2.1. Investigation of Cell Viability When Caspase 8 is Inhibited

To investigate whether NLRP13 overexpression has any effect on caspase-8 dependent cell death mechanism, It was inhibited in one set of our groups. Then cell viability assays were performed again. The cells from all groups were seeded on 6-well as same as before. 2h before the treatment, as recommended in its manual, caspase-8 inhibitor Z-IETD-FMK was given to one set of NLRP13, mCherry and wild-type while an equal volume of DMSO was given to control groups. Inhibitor that we used provide the irreversible inhibition of caspase-8 by preventing its cleavage. In other words, it prevent the enzymatic activation of caspase-8. To confirm this inhibition, LPS/nigericin treatment was performed for both groups and cleavage of caspase-8 was checked by western blotting. No cleaved caspase-8 was detected in caspase-8 inhibited groups while caspase-8 was cleaved in others (Figure 5. 11)

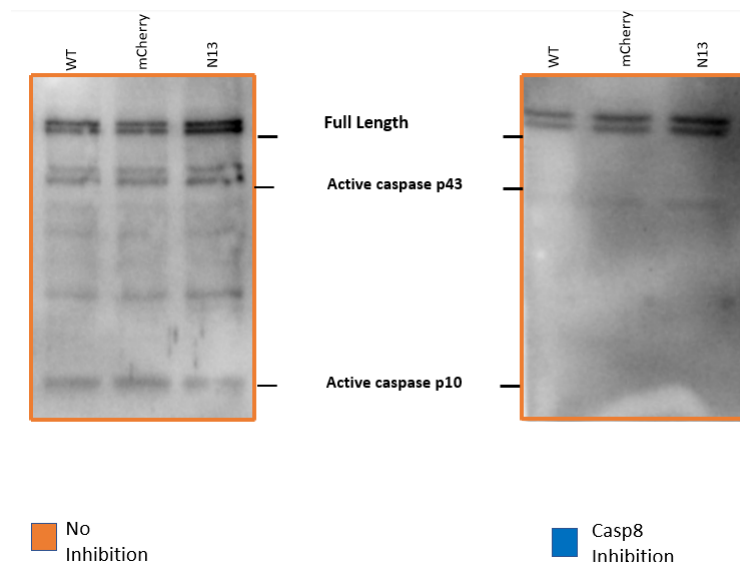


Figure 5.11. Caspase-8 inhibition is confirmed by Western Blotting.

After the confirmation, the medium was removed, and cells were collected gently for Annexin V-PI staining. They were washed with 1X PBS before resuspension in 1X binding buffer. They were incubated with annexin V and PI for 15 min. Flow cytometry was used to read samples. Quadrants are same as given in figure 5.3, 5.4 and 5.5 and percentage of cell death was calculated same way (Q5+Q6+Q7) for each NLRP13 expressing group, mCherry expressing group and wild type group. The cell populations are shown in figure 5.12a. According to the analysis by 2way ANOVA test, percentage of cell death was observed similar for each NLRP13 stable cells, mCherry stable cells and wild type cells. There is no significant difference in cell death (Figure 5.12b).

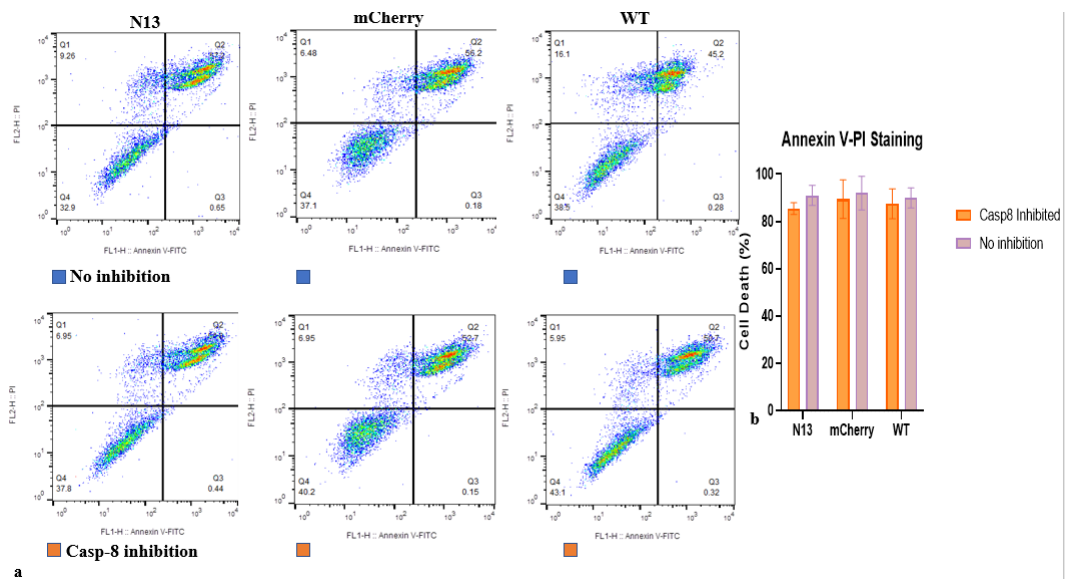


Figure 5.12. Cell Populations and Cell Death Percentages of N13, mCherry and WT. (a) Q5 for PI staining shows the necrotic cell death, Q6 for double staining with PI and annexin V shows late-apoptotic and pyroptotic cell death, Q7 for annexin V staining shows early-apoptotic cell death, Q8 for double negative shows the viable cells. (b) Percentages of treated and untreated cells is calculated as total number of Q5, Q6 and Q7 and Stable NLRP13 expression does not have an effect on cell death when caspase-8 is inhibited. N13: Stably NLRP13 expressing THP-1 cells, mCherry: Stably mCherry expressing THP-1 cells, WT: Wild-Type THP-1 cells.

The collected medium was used to perform an LDH release assay. They were placed into 96-well microplates and the assay was done by following instructions in the manual. LDH percentages were calculated, their LDH release did not change significantly when caspase-8 was inhibited. Furthermore, any significant difference was not observed between caspase-8 inhibited groups which are NLRP13 stable cells, mCherry stable cells and wild-type cells according to 2way ANOVA test (Figure 13).

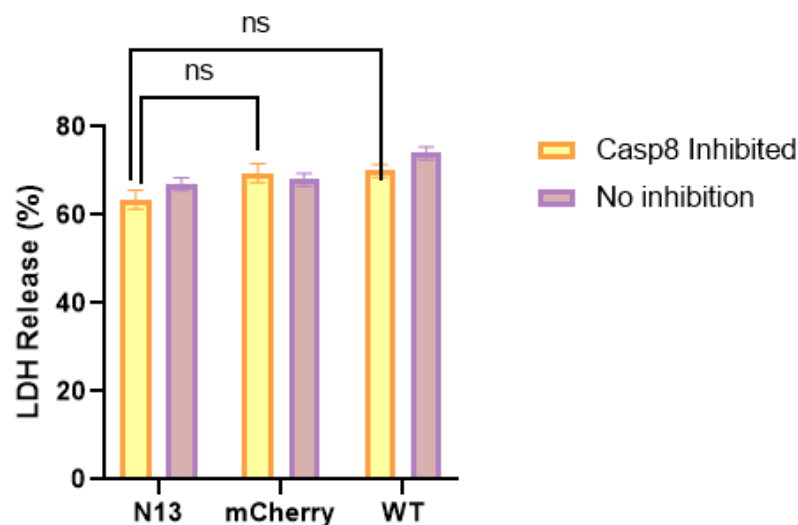


Figure 5.13. Stable NLRP13 expression does not have an effect on the cell death levels when caspase-8 is inhibited

5.2.2. IL1- β Levels upon Pyroptosis in The Absence of Caspase 8

The medium collected from both caspase-8 inhibited and non-inhibited cells was used for ELISA analysis. They were diluted as 1:100 to keep absorbance within the range. Dilutions of them and standards were placed into wells. They were incubated for 2h at room temperature. The detection antibody was prepared at a working concentration when incubation was completed. The samples were removed from the plate. Streptavidin-HRP was added to each well. It was covered to avoid light at this step. After they were read, the secreted IL1- β levels were calculated as picogram (pg). It is shown that there are significant decreases in caspase-8 inhibited groups compared to non-inhibited ones; moreover, its secretion level in the caspase 8 inhibited NLRP13

cells is higher than in caspase 8 inhibited wild-type cells (Figure 14)

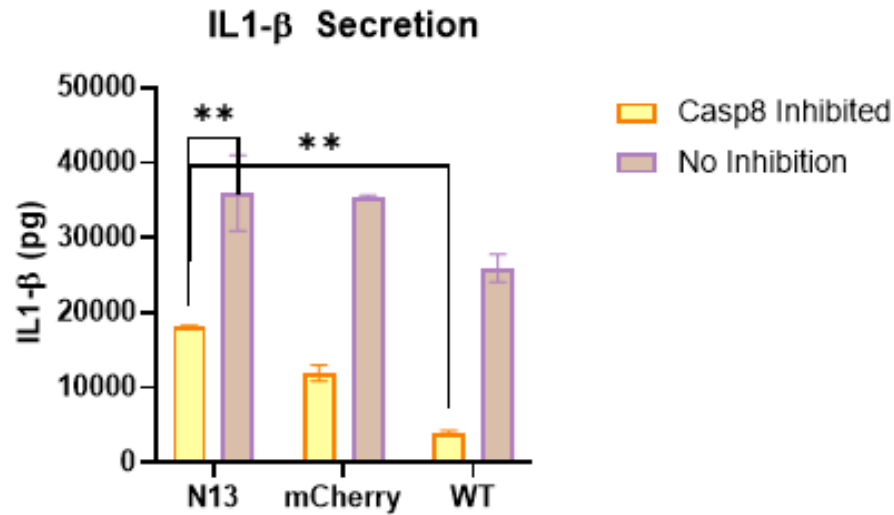


Figure 5.14. IL1- β secretion of NLRP13 overexpressing cells is higher than wild-type cells but not the control cells. N13: Stably NLRP13 expressing THP-1 cells, mCherry: Stably mCherry expressing THP-1 cells, WT: Wild-Type THP-1 cells. **p < 0.01 mean \pm SD

5.2.3. Investigation of Cell Death-Related Proteins in Absence of Caspase8

To observe whether inhibition of caspase can change the cell death-related protein levels in the stably NLRP13 expressing THP-1 cells, Cleaved gasdermin D and PARP-1 proteins were investigated via western blot. The gasdermin D cleavage was still observed in the inhibited cells (Figure 15.a 15b). The protein levels were not different within the inhibited group, however, there is a significant decrease in cleaved gasdermin D level in inhibited cells compared with the non-inhibited cells (Figure 16). Caspase-8 inhibition leads to a decrease in the cleavage of gasdermin D.

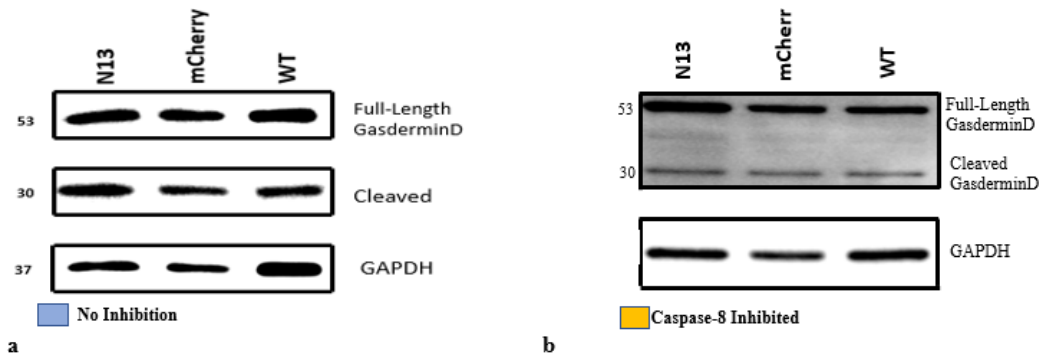


Figure 5.15. Cleavage of gasderminD when caspase-8 is inhibited (a) Protein levels of cleaved gasderminD and full length without caspase-8 inhibition (b) Protein levels of cleaved gasderminD and full length when caspase-8 is inhibited WT. N13: Stably NLRP13 expressing THP-1 cells, mCherry: Stably mCherry expressing THP-1 cells, WT: Wild-Type THP-1 cells.

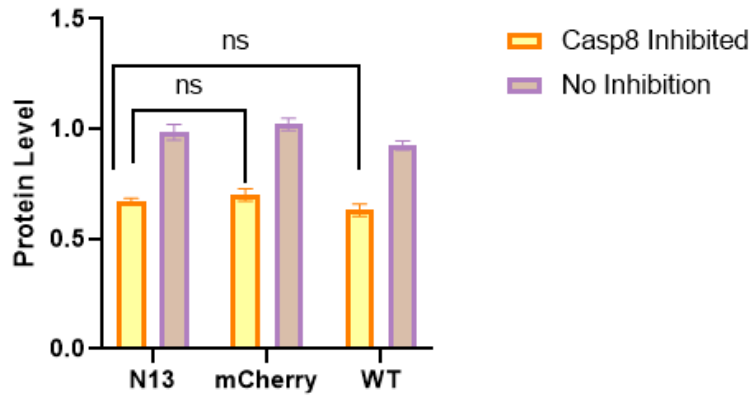


Figure 5.16. Stable NLRP13 expression does not affect the GasderminD protein level when caspase-8 is inhibited.

When the cleavage of PARP-1 was checked (Figure 17a,b) a significant difference was observed in inhibited group compared with the non-inhibited one. Moreover, the cleavage level of PARP-1 was significantly lower than both mCherry and wild-type cells (Figure 18).

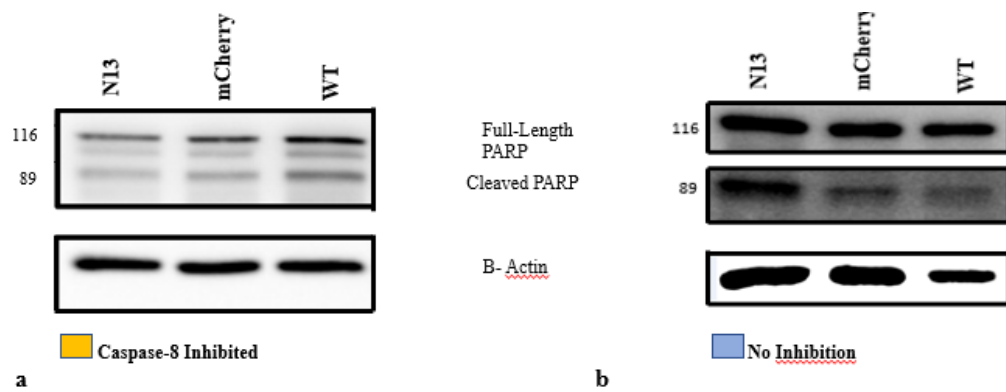


Figure 5.17. PARP-1 cleavage in caspase-8 inhibited cells and noninhibited cells. (a) Protein levels of cleaved PARP-1 and full length in inhibited N13, mCherry and WT. (b) Protein levels of cleaved PARP-1 and full length in noninhibited N13, mCherry and WT. N13: Stably NLRP13 expressing THP-1 cells, mCherry: Stably mCherry expressing THP-1 cells, WT: Wild-Type THP-1 cells.

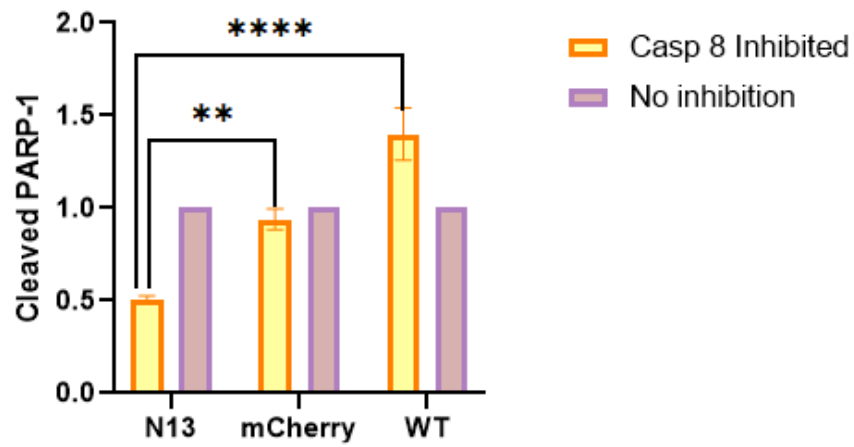


Figure 5.18. Cleavage of PARP-1 in NLRP13 overexpressing cells is slightly lower than control group and significantly lower than WT when caspase-8 is inhibited. N13: Stably NLRP13 expressing THP-1 cells, mCherry: Stably mCherry expressing THP-1 cells, WT: Wild-Type THP-1 cells. * $p \leq 0.05$ **** $p < 0.0001$; mean \pm SD

6. DISCUSSION

NLR family pyrin containing 13, NLRP13, is an intracellular protein that belongs to the NOD-like receptor family. It is known that it is only found in humans, dogs, bovines, and chimpanzees but not in rodents. One paper shows the upregulation of the NLRP13 expression in THP-1 macrophages upon *Toxoplasma gondii* and its survival in coinfection of HIV and tuberculosis. These findings were limited and insufficient to figure out the role of NLRP13 in inflammasome activation. Our lab is pioneer in functional studies of NLRP13. According to their studies, it was already known that NLRP13 is found in the cytosol and partly mitochondria, and it can weakly interact with inflammasome components; caspase-1 and ASC. (Gültekin, 2011) The increase in its expression upon LPS/ATP and *P. Aeruginosa* was also observed previously (Yalçınkaya, 2015; Yilmazer, 2018). Finally, it is known that NLRP13 shows a pro-inflammatory response upon LPS/ATP treatment and *P. Aeruginosa* infection. It was revealed that cleaved subunits p43/p41 and p10 of caspase-8 are higher in the stably NLRP13 expressing THP-1 cells than control cells upon inflammasome activation. This means that activation of procaspase-8 is increased in the stably NLRP13 expressing THP-1 cell. Furthermore, NLRP13 has an interaction with caspase-8 according to Co-IP results. All these findings show that NLRP13 can lead to an increase in the activation of caspase-8 and could be part of the caspase-8 activation complex. (Yilmazer, 2018) It is known that caspase-8 involves in the cell death pathways. It is one of the initiator caspases, and recent studies revealed that it has a crucial role in a molecular switch between pyroptosis, apoptosis, and necrosis. Another study also indicates that caspase-8 can cleave the gasdermin D, which is a significant indicator of pyroptosis, itself. Besides these, NLRP3 inflammasome components such as NLRP3, caspase-1, and ASC are significantly higher in the stably NLRP13 expressing THP-1 cells upon inflammasome activation (Yilmazer, 2018). Since NLRP3 inflammasome activation can induce pyroptosis, it could be thought whether NLRP13 has a role in cell death by involving the caspase-8 activation complex through the inflammasome activation. In this study, the role of the NLRP13 in cell death was investigated.

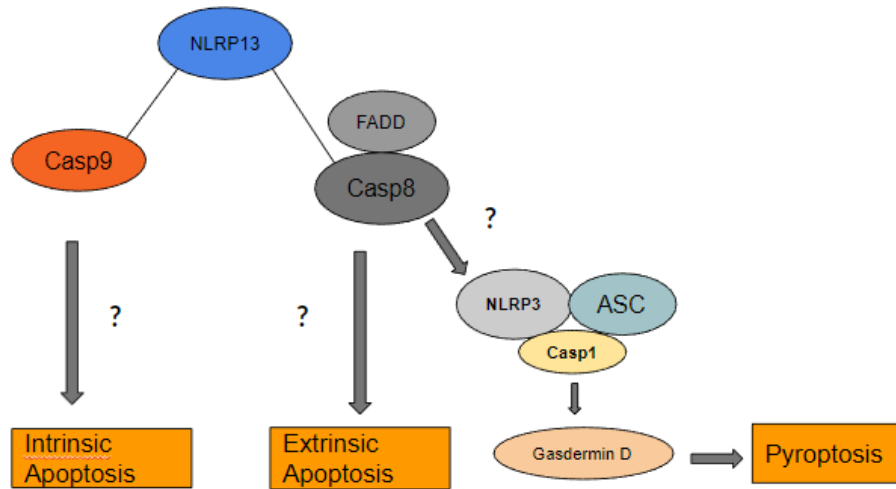


Figure 6.1. Possible Roles of NLRP13 in Cell Death

To investigate the effects of NLRP13 on cell death, NLRP13 expression levels of stably NLRP13 expressing cells were confirmed by western blot. They expressed NLRP13 sufficiently. Stably NLRP13 expressing THP-1 cells, wild-type THP-1 cells, and mCherry expressing THP-1 cells, as a control group, were used for each experimental setup. Firstly, pyroptosis was induced via inflammasome activation. Both treatment and no treatment groups were collected and counted by staining with trypan blue. According to trypan blue staining results, the cell viability of NLRP13 overexpressing THP-1 cells is significantly lower than the control group, mCherry expressing THP-1 cells. There is no significant difference compared to wild-type cells (Figure 5.c). However, trypan blue staining could not be very accurate for cell viability. Therefore, several different assays were used to confirm cell death.

First of all, the LDH levels of each group were checked. Lactate dehydrogenase enzyme (LDH) is a cytosolic enzyme found in all living organisms. When cells die, it releases into the supernatant because of cell membrane damage. (Ka-Ming Chan et al., n.d.) In other words, the level of LDH release correlates with cell death. In our results of LDH release in each group, it was not shown any significant difference (Figure 5.2). However, LDH release occurs only when the membrane is ruptured, as we mentioned before and pore formation occurs in pyroptosis at the beginning of it. In contrast, the

membrane remains intact during apoptosis until secondary necrosis occurs. (Zhang et al., 2018) This means that this data could not reflect all types of cell death. Due to this, Annexin V-PI staining was performed to observe cell death. Only annexin-V stained cells indicate the early-apoptotic stage, while only PI-positive cells indicate the necrotic cell death. Double positive cells show late apoptosis and pyroptosis. When the percentage of cell deaths was compared for each group, any significant difference was not observed (Figure 5.6).

Another significant indicator of inflammasome activation and pyroptosis is IL1- β secretion. It cannot be enough to understand how much cells die, but it provides us with the confirmation of pyroptosis. According to the ELISA results, IL1- β secretion is significantly higher than both wild-type and mCherry (Figure 5.7). In line with cell death findings, this increase could result from the pro-inflammatory effect of NLRP13 since the IL1- β secretion level may not correlate with pyroptosis.

For analysis of cell death mechanisms, cell death-related protein levels were checked in all groups. Gasdermin D is the most crucial indicator of pyroptosis. Cleavage of GasderminD by caspase-1 induces pore formation in the membrane, and pyroptosis occurs.(Zhang et al., 2018) When checking the cleavage of Gasdermin D in treated and untreated groups, cleaved gasdermin D is observed in all treated groups and no cleavage is detected in the untreated groups as expected (Figure 5.8). According to quantification of western blot results, there is no significant difference in protein levels between NLRP13 and control groups (Figure 5.9). This can indicate that NLRP13 does not affect the pyroptosis level significantly.

Then, PARP-1 cleavage was investigated to check the apoptosis. PARP-1 cleavage by caspase-3 is a crucial indicator of apoptosis. (Obeng, 2021) Because of this feature, it is a common apoptosis marker in the literature. The cleaved PARP-1 levels of NLRP13 and control groups show that its cleavage is slightly higher in stably NLRP13 expressing cells than in the control group (Figure 5.10b). When we evaluate it with other results, NLRP13 may have a role in the switch between pyroptosis and apoptosis. Recent studies revealed that the caspase-8 FADD complex is included in the molecular switch

mechanism between cell death.(Fritsch et al., 2019) Maybe, NLRP13 may interact with them and cause a possible switch between apoptosis and pyroptosis. This may explain that there is no significant change in cell viability.

To check whether NLRP13 may have a role in cell death through the caspase-8 activation complex, a caspase-8 inhibitor was given to one set of cells before the treatment. Then, LPS/nigericin treatment was performed. After treatment, cell death assays were repeated for inhibited and non-inhibited control groups. There is no significant difference in LDH release and annexin-V PI staining (Figure 5.12 and 5.13). This means that the cell viability of any group did not change upon caspase-8 inhibition.

However, it was surprisingly observed that IL1- β secretion in all groups was sharply decreased when caspase-8 was inhibited. Even recent studies speculate that caspase-8 could be an inflammatory caspase; this decrease was higher than expected. There is a significant difference between NLRP13 and wild-type but no significant difference between NLRP13 and the control group (Figure 5.14).

Finally, cell death-related protein levels of each group were rechecked. Gasdermin D cleavage was still observed in the caspase-8 inhibited group, as expected, even though their levels were slightly decreased compared with the non-inhibited control group (Figure 5.15a). Recent studies reveal that caspase-8 could play a role in the contribution of inflammasomes, and we also know that it can cleave the gasdermin D itself in the absence of caspase-1(Gram et al., 2019). Thus, caspase-8 can contribute to the cleavage of Gasdermin D, but there is no difference in NLRP13 overexpressing cells (Figure 5.15b). According to the cleavage of PARP-1 in caspase-8 inhibited cells, the most significant decrease was observed in NLRP13 overexpressing cells. The cleaved PARP-1 level in NLRP13 overexpressing cells is significantly lower than in both mCherry and wild-type groups (Figure 5.18). This finding also supports the idea that NLRP13 could play a role molecular switch between apoptosis and pyroptosis with the caspase-8 activation complex.

In line with all these findings, we can conclude that NLRP13 is not involved directly in the pyroptosis with caspase-8. In other words, it could not affect cell viability directly, however, it could lead to inducing pyroptosis earlier. To investigate this, a time-point experimental setup for pyroptosis can be performed. Moreover, cleavage of PARP-1, which is an apoptotic marker, showed that NLRP13 could play a role in the molecular switch mechanism by involving in caspase-8 activation complex. However, these findings cannot be enough to show this themselves. For further investigations, TUNEL assay can be performed to see whether there is a switch into apoptosis or not. Moreover, we still do not know caspase-1 and caspase-9 parts of these possible mechanisms (Figure 6.1). We know that even both caspase-1 and caspase-8 can cleave the gasderminD (Gram et al., 2019), caspase-1 is the main caspase having role in the pyroptosis and inflammation. Thus, these experiments can be repeated while caspase-1 is inhibited to observe to its interaction with NLRP13 during pyroptosis. Previous studies also showed that NLRP13 interact with caspase-9. (Yalçinkaya, 2015) and caspase-9 have a significant role in the intrinsic pathway. (Özören & El-Deiry, 2003) These parts of study could not be performed because of time limitations, however, they can be meaningful to lighten mechanisms that NLRP13 is involved.

7. References

- Biol, T. J., E. Eren and N. Özören, 2019, Turkish Journal of Biology, “The NLRP3 inflammasome: a new player in neurological diseases”, Turkish Journal of Biology Vol. 575, No. 43, pp. 349-359.
- Fritsch, M., S. D. Günther, R. Schwarzer, M. C. Albert, F. Schorn, J. P. Werthenbach, L. M. Schiffmann, N. Stair, H. Stocks, J. M. Seeger, M. Lamkanfi, M. Krönke, M. Pasparakis and H. Kashkar, 2019, “Caspase-8 Is the Molecular Switch for Apoptosis, Necroptosis and Pyroptosis”, Nature, Vol. 575, No. 7784, pp. 683–687.
- Galluzzi, L., I. Vitale, S. A. Aaronson, J. M. Abrams, D. Adam, P. Agostinis, E. S. Alnemri, L. Altucci, I. Amelio, D. W. Andrews, M. Annicchiarico-Petruzzelli, A. V. Antonov, E. Arama, E. H. Baehrecke, N. A. Barlev, N. G. Bazan, F. Bernassola, M. J. M. Bertrand, K. Bianchi, M. V. Blagosklonny, K. Blomgren, C. Borner, P. Boya, C. Brenner, M. Campanella, E. Candi, D. Carmona-Gutierrez, F. Cecconi, F. K. M. Chan, N. S. Chandel, E. H. Cheng, J. E. Chipuk, J. A. Cidlowski, A. Ciechanover, G. M. Cohen, M. Conrad, J. R. Cubillos-Ruiz, P. E. Czabotar, V. D’Angiolella, T. M. Dawson, V. L. Dawson, V. De Laurenzi, R. De Maria, K. M. Debatin, R. J. Deberardinis, M. Deshmukh, N. Di Daniele, F. Di Virgilio, V. M. Dixit, S. J. Dixon, C. S. Duckett, B. D. Dynlacht, W. S. El-Deiry, J. W. Elrod, G. M. Fimia, S. Fulda, A. J. García-Sáez, A. D. Garg, C. Garrido, E. Gavathiotis, P. Golstein, E. Gottlieb, D. R. Green, L. A. Greene, H. Gronemeyer, A. Gross, G. Hajnoczky, J. M. Hardwick, I. S. Harris, M. O. Hengartner, C. Hetz, H. Ichijo, M. Jäättelä, B. Joseph, P. J. Jost, P. P. Juin, W. J. Kaiser, M. Karin, T. Kaufmann, O. Kepp, A. Kimchi, R. N. Kitsis, D. J. Klionsky, R. A. Knight, S. Kumar, S. W. Lee, J. J. Lemasters, B. Levine, A. Linkermann, S. A. Lipton, R. A. Lockshin, C. López-Otín, S. W. Lowe, T. Luedde, E. Lugli, M. MacFarlane, F. Madeo, M. Malewicz, W. Malorni, G. Manic, J. C. Marine, S. J. Martin, J. C. Martinou, J. P. Medema, P. Mehlen, P. Meier, S. Melino, E. A. Miao, J. D. Molkenin, U. M. Moll, C. Muñoz-Pinedo, S. Nagata, G. Nuñez, A. Oberst, M. Oren, M. Overholtzer, M. Pagano,

T. Panaretakis, M. Pasparakis, J. M. Penninger, D. M. Pereira, S. Pervaiz, M. E. Peter, M. Piacentini, P. Pinton, J. H. M. Prehn, H. Puthalakath, G. A. Rabinovich, M. Rehm, R. Rizzuto, C. M. P. Rodrigues, D. C. Rubinsztein, T. Rudel, K. M. Ryan, E. Sayan, L. Scorrano, F. Shao, Y. Shi, J. Silke, H. U. Simon, A. Sistigu, B. R. Stockwell, A. Strasser, G. Szabadkai, S. W. G. Tait, D. Tang, N. Tavernarakis, A. Thorburn, Y. Tsujimoto, B. Turk, T. Vanden Berghe, P. Vandenabeele, M. G. Vander Heiden, A. Villunger, H. W. Virgin, K. H. Vousden, D. Vucic, E. F. Wagner, H. Walczak, D. Wallach, Y. Wang, J. A. Wells, W. Wood, J. Yuan, Z. Zakeri, B. Zhivotovsky, L. Zitvogel, G. Melino and G. Kroemer, 2018, “Molecular Mechanisms of Cell Death: Recommendations of the Nomenclature Committee on Cell Death 2018”, *Cell Death and Differentiation*, Vol. 25, No. 3, pp. 486–541.

Gram, A. M., L. M. Booty and C. E. Bryant, 2019, “Chopping GSDMD: Caspase-8 Has Joined the Team of Pyroptosis-mediating Caspases”, *The EMBO Journal*, Vol. 38, No. 10, pp. 2–4.

Guo, H., J. B. Callaway and J. P. Y. Ting, 2015, “Inflammasomes: Mechanism of Action, Role in Disease, and Therapeutics”, *Nature Medicine*, Vol. 21, No. 7, pp. 677–687.

Gültekin Y., 2011, Cloning and Characterization of Novel Nod Like Receptors as Cytoplasmic Immune Sensors, M.S. Thesis, Boğaziçi University.

Ha, M. S., M. S. Jeong and S. B. Jang, 2021, “Structural and Functional Roles of Caspase-8 in Extrinsic Apoptosis”, *Journal of Life Science*, Vol. 31, No. 10, pp. 954–959.

Han, J.-H., J. Park, T.-B. Kang and K.-H. Lee, 2021, *Molecular Sciences*, “Regulation of Caspase-8 Activity at the Crossroads of Pro-Inflammation and Anti-Inflammation”, Vol. 22, No. 10, pp. 3318–3324.

He, Y., H. Hara and G. Núñez, 2016, “Mechanism and Regulation of NLRP3 Inflamma-

some Activation”, *Trends in Biochemical Sciences*, Vol. 41, No. 12, pp. 1012–1021.

Ka-Ming Chan, F., K. Moriwaki and M. José De Rosa, 2013, “Detection of Necrosis by Release of Lactate Dehydrogenase (LDH) Activity”, *Methods Mol Biol*, Vol. 979, No. 12, pp. 65-70.

Kesavardhana S., R. K. S. Malireddi, and T. D. Kanneganti, 2020, “Caspases in Cell Death, Inflammation, and Pyroptosis.” *Annual Review of Immunology*, Vol. 38, No. 1, pp. 567–595.

Latz, E., T. Sam Xiao and A. Stutz, 2013, “Activation and regulation of the inflammasomes”, *Nature Immunology*, Vol. 13, No. 12, pp. 397-409.

Li, J., and J. Yuan, 2008, “Caspases in Apoptosis and Beyond”, *Oncogene*, Vol. 27, No. 48, pp. 6194–6206.

Maes, M., T. Vanhaecke, B. Cogliati, S. C. Yanguas, J. Willebrords, V. Rogiers and M. Vinken, 2015, “Measurement of apoptotic and necrotic cell death in primary hepatocyte cultures”, *Methods Mol Biol*, Vol. 1250, No. 10, pp. 349-361.

McIlwain, D. R., T. Berger and T. W. Mak, 2013, “Caspase Functions in Cell Death and Disease”, *Cold Spring Harbor Perspectives in Biology*, Vol. 5, No. 4, pp. 1–28.

Obeng, E., 2021, “Apoptosis (Programmed Cell Death) and Its Signals-a Review”, *Brazilian Journal of Biology*, Vol. 81, No. 4, pp. 1133–1143.

Özören, N., and W. S. El-Deiry, 2003, “Cell Surface Death Receptor Signaling in Normal and Cancer Cells”, *Seminars in Cancer Biology*, Vol. 13, No. 2, pp. 135–147.

Shen, C., J. Pei, X. Guo, L. Zhou, Q. Li and J. Quan, 2018, “Structural Basis for Dimerization of the Death Effector Domain of the F122A Mutant of Caspase-8”, *Scientific Reports*, Vol. 8, No. 1, pp. 1–10.

- Tang, D., R. Kang, T. Vanden Berghe, P. Vandenabeele and G. Kroemer, 2019, “The Molecular Machinery of Regulated Cell Death”, *Cell Research*, Vol. 29, No. 5, pp. 347–364.
- Ting J. P. Y., R. C. Lovering, E. S. Alnemri, J. Bertin, J. M. Boss, B. K. Davis, R. A. Flavell, S. E. Girardin, A. Godzik, J. A. Harton, H. M. Hoffman, J. P. Hugot, N. Inohara, A. MacKenzie, L. J. Maltais, G. Nunez, Y. Ogura, L. A. Otten, D. Philpott, P. A. Ward, 2008, “The NLR Gene Family: A Standard Nomenclature.” *Immunity*, Vol. 28, No. 3, pp. 285–287.
- Tummers, B., and D. R. Green, 2017, “Caspase-8: Regulating Life and Death”, *Immunological Reviews*, Vol. 277, No. 1, pp. 76–89.
- Yağcınkaya M., 2015, Characterization of NLRP13 in Inflammasome Activity, M.S. Thesis, Boğaziçi University.
- Yılmaz A., 2018, Investigation of NLRP13-Driven Innate Immune Responses, M.S. Thesis, Boğaziçi University.
- Yu, P., X. Zhang, N. Liu, L. Tang, C. Peng and X. Chen, 2021, “Pyroptosis: Mechanisms and Diseases”, *Signal Transduction and Targeted Therapy*, Vol. 6, No. 1.
- Zhang, Y., X. Chen, C. Gueydan and J. Han, 2018 “Plasma Membrane Changes during Programmed Cell Deaths”, *Cell Research*, Vol. 28, , pp. 9–21.
- Zheng, D., T. Liwinski and E. Elinav, 2020a, “Inflammasome Activation and Regulation: Toward a Better Understanding of Complex Mechanisms”, *Cell Discovery*, Vol. 6, No. 1 pp. 1-22.
- Zheng, D., T. Liwinski and E. Elinav, 2020b “Inflammasome Activation and Regulation: Toward a Better Understanding of Complex Mechanisms”, *Cell Discovery*, Vol. 6, No. 1 pp. 26-33.

Zhong, Y., A. Kinio, M. Saleh, T. A. Kufer and A. Mansell, 2013, "Functions of NOD-like receptors in human diseases", *Frontiers in Immunology*, Vol. 4, No. 1 pp. 1-11.